PHILOSOPHICAL TRANSACTIONS OF THE ROYAL SOCIETY B BIOLOGICAL SCIENCES

Tentacle Autotomy in the Hydromedusa Aglantha digitale (Cnidaria): An Ultrastructural and Neurophysiological Analysis

L. R. Bickell-Page and G. O. Mackie

Phil. Trans. R. Soc. Lond. B 1991 **331**, 155-170
doi: 10.1098/rstb.1991.0005

Tentacle autotomy in the hydromedusa *Aglantha digitale* (Cnidaria): an ultrastructural and neurophysiological analysis

L. R. BICKELL-PAGE AND G. O. MACKIE

Department of Biology, University of Victoria, Victoria, British Columbia, Canada V8W 2Y2

SUMMARY

Tentacles of the hydromedusa *Aglantha digitale* readily detach (autotomize) at a predictable site (autotomy plane) when a tentacle is pinched and tugged. The response is reversibly inhibited in seawater containing excess Mg^{2+}. Behavioural, electrophysiological and ultrastructural analyses indicate that passive and active processes are involved in tentacle autotomy. Inherent structural weakness at the tentacle autotomy plane is suggested by thinning of mesoglea and reduction of muscle tails at this site. The autotomy plane is also characterized by a ring of distinctive ectodermal cells with vacuoles concentrated along the basal cell membrane bordering the mesoglea. These vacuolated autotomy plane (VAP) cells are extensively innervated and, except for a few slender muscle tails, they interrupt the sheath of myoepithelium encasing each tentacle. Tentacles fixed after an autotomizing stimulus but before tentacle breakage show loss of basal vacuoles in VAP cells and holes in the underlying mesoglea. We suggest that the active mechanisms for tentacle autotomy include strong contraction of muscle tails on either side of the autotomy plane and activation of VAP cells, which somehow lower the tensile strength of autotomy plane mesoglea.

Autotomizing stimuli do not appear to evoke a special conduction system within the tentacle. High-frequency nerve-impulse activity in the tentacle conduction system that otherwise directs graded tentacle contractions is initiated by autotomizing stimuli and precedes tentacle disjunction.

Tentacle autotomy in *Aglantha*, a delicate holopelagic hydromedusa that inhabits densely populated pelagic zones, may allow escape when the tentacles inadvertently entangle and overly large and potentially damaging zooplankters.

INTRODUCTION

Defensive autotomy is characterized by a rapid, intrinsically controlled detachment of a body part for the purpose of defence or escape (Frédéricq 1883; see Stasek (1967) and Emson & Wilkie (1980) for discussions of definition). Detachment occurs at a predictable site and is initiated by a threatening external stimulus. The behaviour is widespread and detachment mechanisms have been studied in echinoderms (reviewed by Emson & Wilkie 1980; Wilkie 1984; Wilkie & Emson 1988), crustaceans (reviewed by McVean 1982), molluscs (see Hodgson 1984; Bickell-Page 1989), and chordates (see Wake & Dresner 1967; Sheppard & Bellairs 1972). Although cnidarians offer many examples of tissue separation for asexual reproduction, reports of defensive autotomy in the Cnidaria are few. However, bracts and nectophores of physonectid siphonophores such as *Nanomia* detach readily after a pinch by forceps, and preliminary observations suggest muscle contraction about the autotomy plane is involved (Mackie *et al.* 1987). Purcell (1977) reported that tips of defensive ('catch') tentacles of the anemone *Metridium senile* adhere to an adjacent anemone by nematocyst discharge and subsequently autotomize.

Tentacles of the holopelagic hydromedusa *Aglantha digitale* (O. F. Müller 1776) detach easily at a predictable basal site (autotomy plane) when given a firm, maintained pinch accompanied by a slight tug. This species is also notable for its ability to perform escape swimming as well as normal slow swimming (Singla 1978; Mackie 1980; Roberts & Mackie 1980; Weber *et al.* 1982; Kerfoot *et al.* 1985; Mackie & Meech 1985). Autotomy is only one of several unusual features exhibited by *Aglantha* tentacles: the myoepithelial cells are striated, a giant axon extends down the length of each tentacle, and multiciliated cells occur along two lateral rows (Roberts & Mackie 1980; Mackie *et al.* 1989). In the present study we used electron microscopical and electrophysiological methods to investigate the mechanism and control of tentacle autotomy in *Aglantha*.

We suggest that tentacle autotomy is accomplished by a combination of built-in structural weakness at the autotomy plane and active breakage mechanisms induced by long-lasting, high-frequency nerve-impulse activity in a tentacle conduction system that otherwise controls graded tentacle movements. The active mechanisms involved are strong, sustained contraction of two tentacle muscle systems and, possibly, activation of unique vacuolated ectodermal cells that encircle the

Phil. Trans. R. Soc. Lond. B (1991) **331**, 155–170
Printed in Great Britain

autotomy plane. Both mechanisms appear to target the mesoglea of the autotomy plane, which becomes fenestrated following potentially autotomizing stimuli.

MATERIALS AND METHODS

Aglantha digitale were collected from around the docks of the Friday Harbor Laboratories, University of Washington, U.S.A., and from the Oak Bay Marina, Victoria, Canada, during the spring months of 1987 and 1988. Hydromedusae were kept at 10 °C in screwcap glass bottles.

(*a*) *Electron microscopy*

Aglantha were anaesthetized in five parts ambient seawater and one part isotonic (67 g l^{-1}) magnesium chloride (MgSW) for several minutes. A short segment of bell margin was excised and pinned to a thin block of Sylgard (Dow Corning). To prevent curling of the tentacle bases and bell margin during fixation, several spines (glochids) from the cactus *Opuntia* were inserted in the Sylgard along a line parallel to the bell margin and tentacles were wrapped around the spines.

Anaesthetized chunks of bell margin bearing unpinched, intact tentacles were placed directly into primary fixative. To obtain pinched but still intact tentacles, chunks of bell margin, prepared as described, were transferred into normal seawater for 4–5 min. and all non-secured tentacles were pinched to cause autotomy. Secured tentacles were then pinched strongly but briefly and without tugging, which tended to leave them intact. After 1–2 min. the mounted tissue was transferred to MgSW for 1–2 min. before fixation. Frequently, tentacles in this category broke at the autotomy plane during later processing for electron microscopy. Finally, tentacles were autotomized in normal seawater and both the detached tentacle and the bell margin bearing the broken tentacle bases were fixed.

The primary fixative was glutaraldehyde (2.5 % by volume) in 0.2 M Millonig's phosphate buffer (pH 7.6) with sodium chloride added to raise the osmolality to 940 mosmols† (Cloney & Florey 1968). Tissues were left in primary fixative for one to four days, followed by several rinses in sodium bicarbonate (25 g l^{-1}) (pH 7.2) and post-fixation for 1 h in a 1:1 mixture of osmium tetroxide (40 g l^{-1}) and sodium bicarbonate buffer. In some cases, tissues were cut from Sylgard blocks while in 70 % ethanol during alcohol dehydration. Alternatively, we used acetone to dehydrate mounted tissue, floated the blocks tissue side down on the surface of liquid Epon 812, and subsequently peeled the Sylgard from the surface of the polymerized plastic containing the tissue.

The autotomy planes of 18 tentacles were sectioned to varying extents: 7 unpinched intact tentacles, 9 pinched intact tentacles and 2 stumps of tentacle base after tentacle autotomy. Sections were stained in uranyl acetate followed by lead citrate. Three unpinched intact tentacles were semiserially cross sectioned from approximately 50 μm proximal to the autotomy plane, through to 40–50 μm into the tentacle shaft. At least one tentacle profile per micrometre of tentacle length (more in critical areas) was photographed at a magnification of 873 × (on the negative) with a Philips EM 300 and a photographic composite was constructed of each profile.

† One osmole contains one mole of osmotically active particles.

(*b*) *Electrophysiology*

Electrophysiological records were made using fine polyethylene suction electrodes for stimulating and recording extracellularly, and glass micropipettes filled with 3 M KCl for intracellular recording. Standard stimulators and amplifiers were used, and display was on a storage oscilloscope or chart recorder. Except for figure 35*a*, which is from a chart recording, all figures were photographed from the oscilloscope screen.

RESULTS

(*a*) *General tentacle structure and autotomy behaviour*

The many tentacles extending from the bell margin of *Aglantha* consist of a central column of endodermal cells stacked end-on-end, an outer investment of ectoderm composed mostly of epitheliomuscle cells with muscle tails oriented at a slight angle to the tentacle long axis, and a thin layer of fibrous mesoglea between the two cellular layers. Mackie *et al.* (1989) identified three regions along the length of each tentacle: the base, shaft and whip. The autotomy plane lies between the thick, short tentacle base and the thinner, longer shaft (figure 1). The larger diameter of the tentacle base is due to a greater thickness of myoepithelium, particularly along the oral aspect, and to prominent tracts of ectodermal sensory cells extending longitudinally down the lateral and oral sides of the tentacle base (Arkett *et al.* 1988). Other ectodermal components include cnidocytes and a pair of motile ciliary tracts along the shaft and whip. The diameter of the endoderm is approximately the same throughout the tentacle (figure 1).

The tentacles are highly mobile and capable of independent movements and characteristic coordinated movements during whole animal behaviours such as fishing ('slow swimming'), feeding and escape swimming (Donaldson *et al.* 1980; Roberts & Mackie 1980; Mackie *et al.* 1989). In response to a pinch or electrical shock, an individual tentacle shows a gradient of responses dependent on the strength of the stimulus. Very weak stimuli produce local tentacle shortening, manifested as a coiling of the tentacle in the stimulated region, and local arrest of cilia. Stronger stimuli cause abrupt coiling of the entire tentacle distal to the base, flexion of the tentacle base toward the bell cavity, and total arrest of tentacle cilia (Mackie 1980; Mackie *et al.* 1989). Sustained, crushing pinches produce strong contraction of the tentacle, a series of rapid contractions of the bell (the escape swim), and detachment of the tentacle at the autotomy plane. Neighbouring tentacles do not autotomize unless also pinched firmly.

Microscopic observations on pinned medusae show a

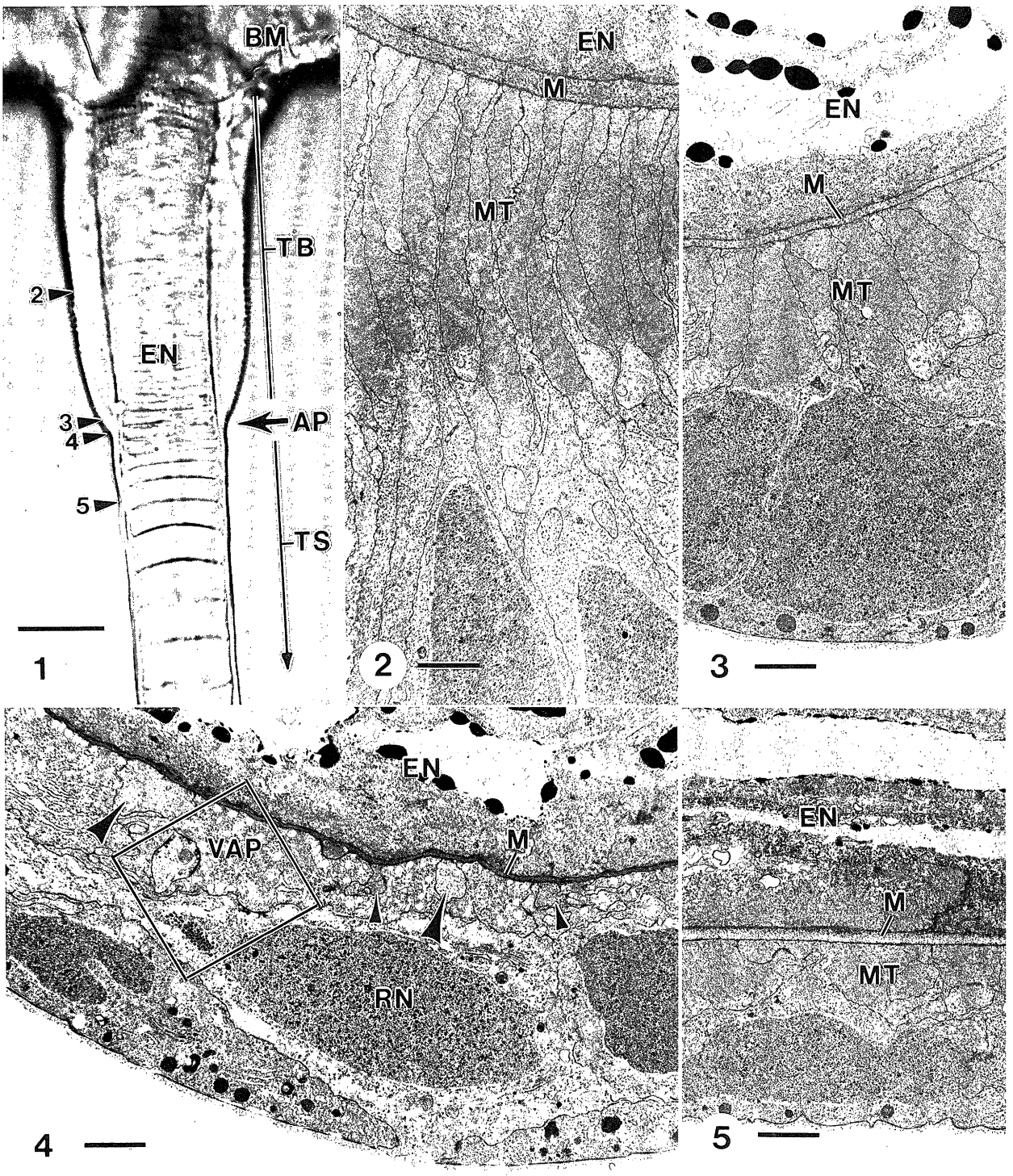

Figure 1. Photomicrograph of a tentacle base (TB) attached to the bell margin (BM), tentacle shaft (TS), and autotomy plane (AP). EN, endoderm. Numbered arrowheads indicate levels of cross sections shown in figures 2–5. Scale bar 50 μm.

Figures 2–5. Cross sections of epitheliomuscle cells on oral side of tentacle at four different levels. EN, endoderm; M, mesoglea; MT, muscle tails. Scale bars 2 μm.

Figure 2. Midway along tentacle base; muscle tails shaped as broad ribbons.

Figure 3. Extreme distal end of tentacle base.

Figure 4. Autotomy plane; vacuolated autotomy plane cells (VAP) surround small, isolated muscle tails extending from the tentacle base (small arrowheads) and from the tentacle shaft (large arrowheads). Note thin mesoglea. Boxed area enlarged in figure 24. RN, ring neuron.

Figure 5. Tentacle shaft approximately 20 μm distal to autotomy plane.

PHILOSOPHICAL TRANSACTIONS OF THE ROYAL SOCIETY B BIOLOGICAL SCIENCES

slight constriction at the autotomy plane immediately after a tentacle is pinched. This appearance is created by bulging of tissues on either side of the autotomy plane. The subsequent disjunction occurs as a clean, abrupt separation of tissues. For pinned medusae, autotomy is greatly facilitated by holding the tentacle under slight tension during pinching; detachment typically requires 3–5 s, occasionally longer. Tentacles are particularly easy to detach if they are tugged 1–2 min. after an initial strong pinch.

Medusae anaesthetized in MgSW fail to show tentacle autotomy after stimulus strengths more than sufficient to cause autotomy in unanaesthetized animals. The effect is reversible. Anaesthetized tentacles will eventually detach if given a very strong, sustained pull. Tentacles autotomized less readily and occasionally broke outside the autotomy plane in unanaesthetized animals held for longer than one to two days in the laboratory. The shaft and whip of unanaesthetized tentacles, which have diameters similar to the autotomy plane region, show great resistance to rupture if stretched between two forceps and the eventual tear is ragged.

(*b*) *Ultrastructure of unpinched intact tentacle*

(i) *Ectoderm*

Down the entire length of the tentacle, the muscle field along the oral side is thicker than that along the aboral side. This difference is most pronounced at the tentacle base, where cell bodies of epitheliomuscle cells on the oral side are columnar in shape and are connected to two or more ribbon-shaped muscle tails. The ribbons are packed together along their broad sides to produce a very thick muscle layer along the oral aspect of the tentacle base (figure 2).

As seen in cross sections through the tentacle base, the depth and absolute number of muscle tails gradually diminish toward the autotomy plane (compare figures 2 and 3). At the autotomy plane, most of the muscle tails terminate abruptly so that only a few isolated and slender muscle tails extend into the autotomy plane from the tentacle base (figure 4). Within the tentacle shaft, muscle tails are approximately square in cross section and connect to cuboidal cell bodies (figure 5). As on the proximal side of the autotomy plane, only occasional muscle tails originating within the tentacle shaft penetrate into the autotomy plane region (figure 4).

Microscope observations of live tentacles show clearly a striation pattern within tentacle muscle tails (figure 5*c* of Roberts & Mackie (1980)). Nevertheless, the ultrastructure of tentacle muscle is quite different from that of the cross striated muscle tails of the subumbrellar ectoderm of *Aglantha* (Singla 1978). Longitudinal sections fail to show cross striations in tentacle muscle tails, although cross sections reveal alternating arrays of thick and thin myofilaments (figure 6). We conclude that the tentacle muscle is obliquely striated. Adherens junctions connect neighbouring muscle tails (figure 7) and gap junctions also occur between epitheliomuscle cells (Mackie *et al.* 1989). On either side of the autotomy plane, muscle tails occasionally send slender processes across the mesoglea to underlying endodermal cells (figure 8). We cannot say if similar transmesogleal extensions occur elsewhere along the tentacle.

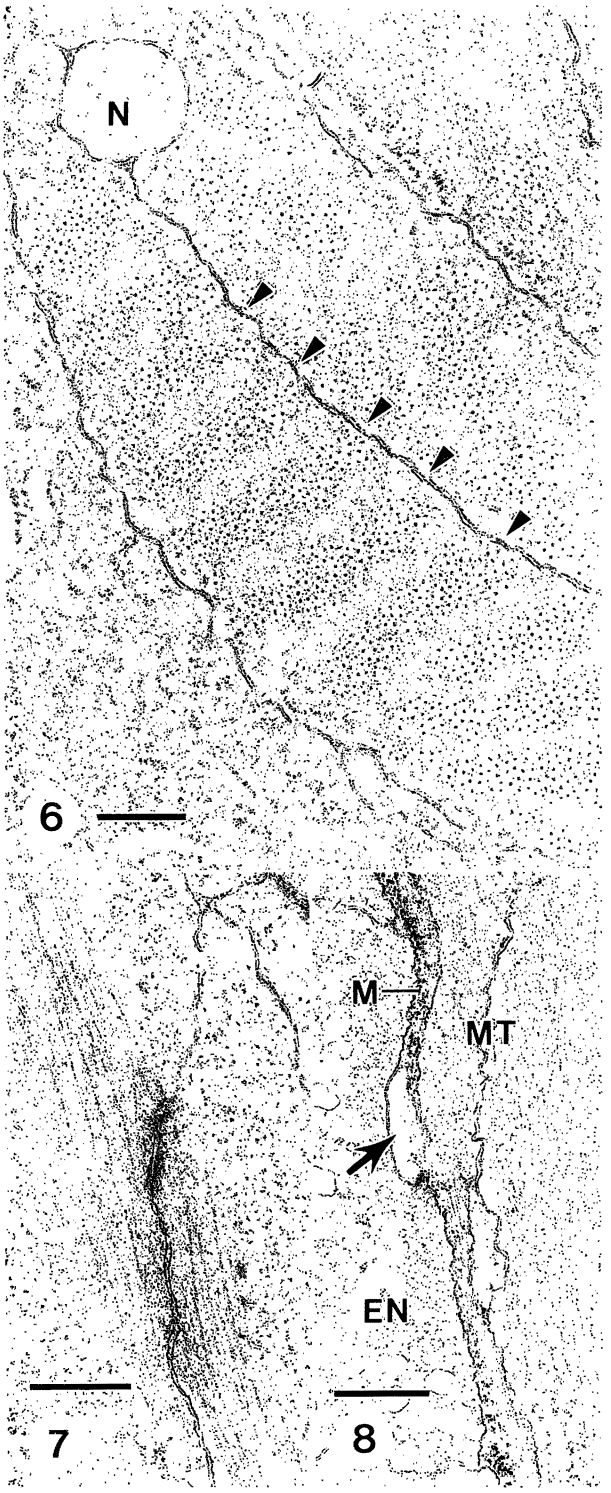

Figure 6. Cross section through a muscle tail showing alternating zones of thick (arrowheads) and thin filaments. N, small neurite. Scale bar 0.5 μm.
Figure 7. Adherens junction between adjacent muscle tails. Scale bar 0.5 μm.
Figure 8. Cytoplasmic process (arrow) from a muscle tail (MT) extending across mesoglea (M) just distal to autotomy plane. EN, endoderm. Scale bar 0.5 μm.

PHILOSOPHICAL TRANSACTIONS OF THE ROYAL SOCIETY B BIOLOGICAL SCIENCES

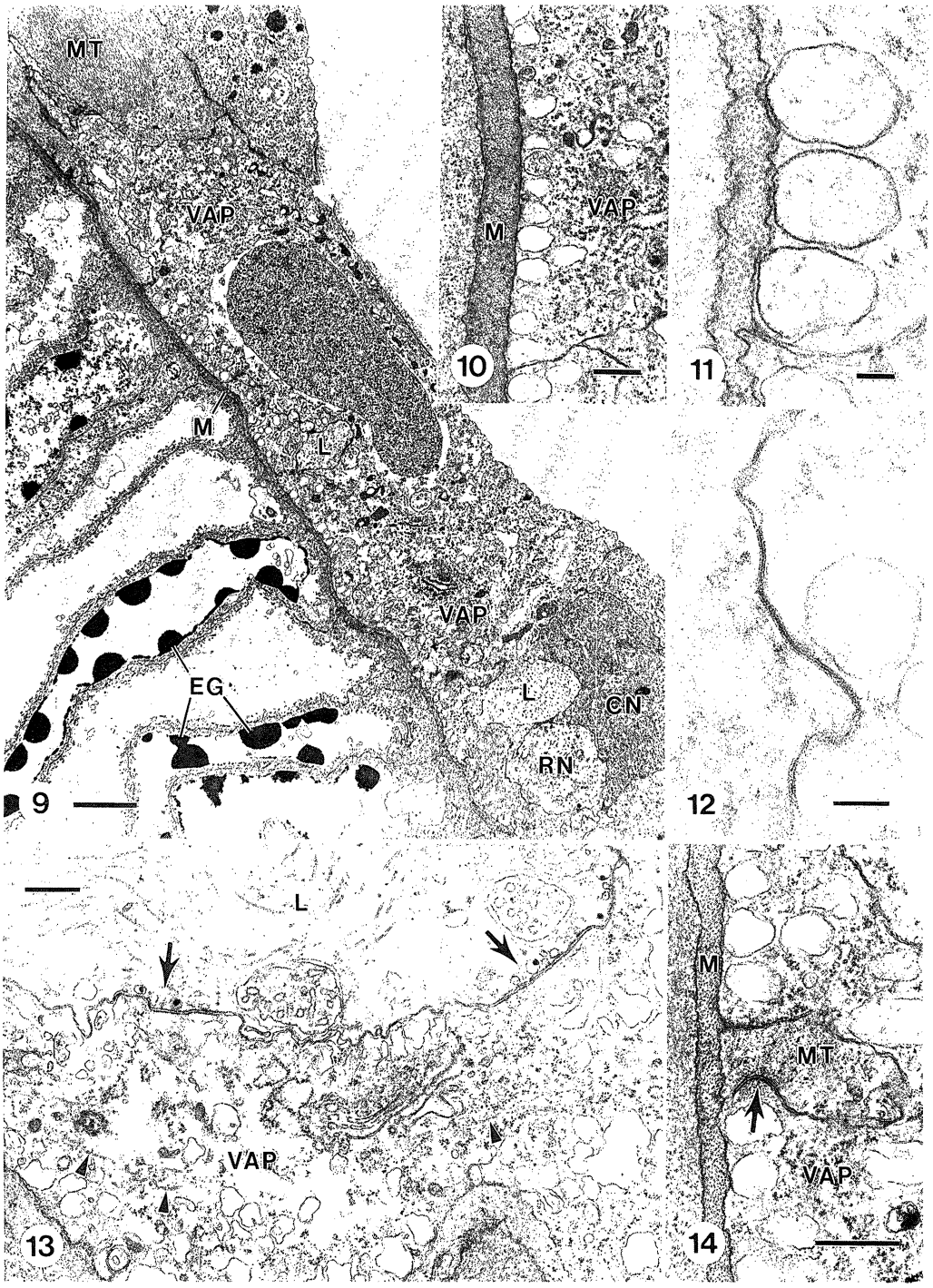

Figure 9. Longitudinal section through the autotomy plane on oral side of tentacle. Muscle tails (MT) from tentacle base abut with vacuolated autotomy plane cell (VAP) with vacuoles concentrated towards thin mesoglea (M). Section passes through two branches of a lateral neurite (L) from a giant tentacle neuron and a neurite from a ring neuron (RN). CN, cnidocyte; EG, endodermal granules. Scale bar 2 μm.

Figure 10. Longitudinal section showing vacuoles of VAP cells lined-up along basal membrane adjacent to mesoglea (M). Scale bar 0.5 μm.

Figure 11. Detail of VAP vacuoles adjacent to basal cell membrane. Scale bar 0.1 μm.

Figure 12. Gap junction between VAP cells. Scale bar 0.1 μm.

Figure 13. Longitudinal, tangential section through the autotomy plane showing synaptic sites (arrows) between a lateral neurite (L) of a giant tentacle neuron and VAP cell. Arrowheads indicate microtubules. Scale bar 0.5 μm.

Figure 14. Adherens junction (arrow) between a small muscle tail (MT) and a VAP cell. M, mesoglea. Scale bar 0.5 μm.

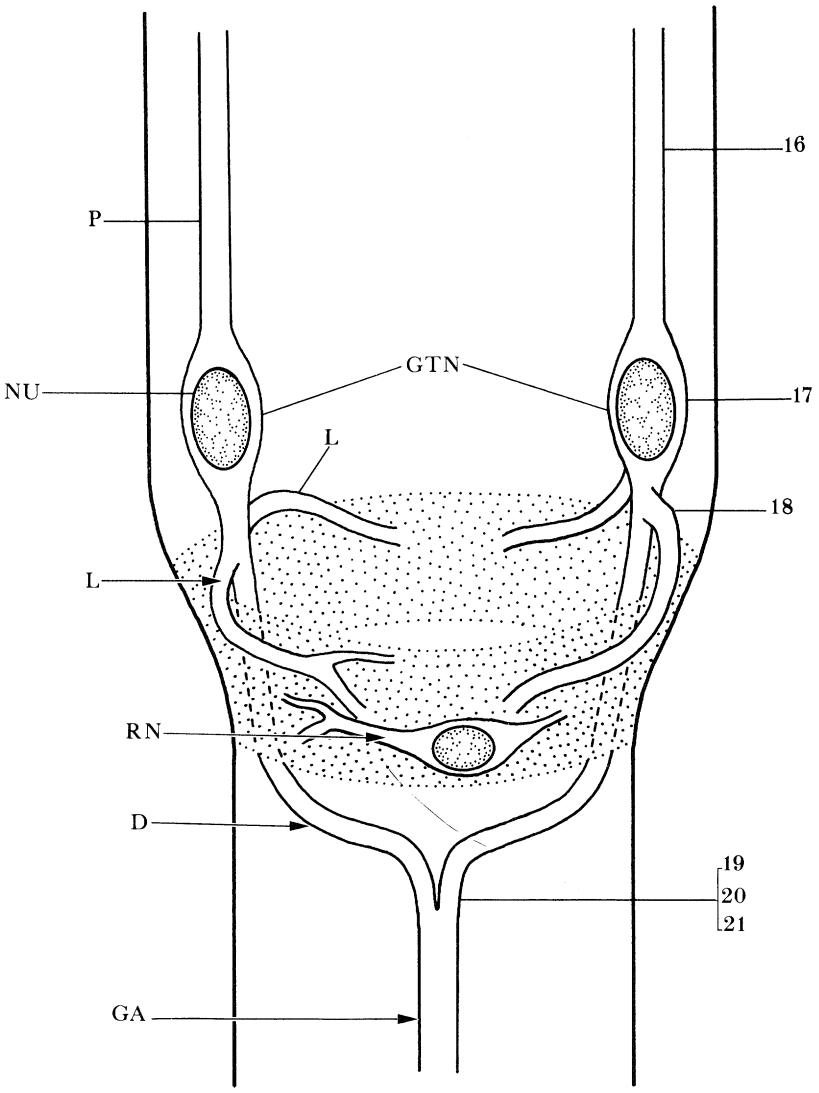

Figure 15. Sketch of giant tentacle neurons (GTN). Stippling represents zone of VAP cells. The numbered arrows refer to sites of cross sections shown in figures 16–21. Drawing not to scale. Abbreviations: D, distal neurite; GA, giant axon; L, lateral neurites; NU, nucleus; P, proximal neurite; RN, ring neuron (only one shown).

The small, isolated muscle tails that extend into the autotomy plane are surrounded by a unique type of cell that collectively form a ring circumscribing the tentacle at the autotomy plane. This ring of vacuolated autotomy plane cells (VAP cells) is one to two cells wide and imposes a structural discontinuity in the sheet of epitheliomuscle cells encasing the tentacle (figure 9). In many respects, the cytoplasm of VAP cells is similar to perinuclear cytoplasm of epitheliomuscle cells. However, small membrane-bounded vacuoles (typical diameter 350 nm) are concentrated within the basal cytoplasm of VAP cells; in particular, many vacuoles are lined-up along the basal membrane bordering the mesoglea (figures 10 and 11). The vacuoles appear empty except for a diffuse flocculent material (figure 11). Microtubules, mainly oriented longitudinally, and two to four Golgi bodies are also present within the cytoplasm (figure 13) and VAP cells are interconnected by gap junctions (figure 12). Semiserial longitudinal and cross sections repeatedly confirmed that VAP cells do not give rise to muscle tails either proximally or distally from the autotomy plane, yet VAP cells are extensively innervated as described below.

Muscle tails extending distally into the autotomy plane from the tentacle base and proximally from the tentacle shaft do not typically span the entire zone of VAP cells (several exceptions found), but form small adherens junctions onto VAP cells before terminating (figure 14).

(ii) *Nerve tracts and neurons*

Two prominent nerve tracts extend into each tentacle from the outer nerve ring of the bell margin. The tracts are located within the ectoderm and run down each side of the tentacle base. Immediately distal to the autotomy plane, the two tracts swing aborally, and eventually come together to form a single tract that runs along the aboral side of the remainder of the tentacle. As sketched in figure 15, each nerve tract within the tentacle base includes a large neurite (figure 16) that arise separately from a pair of large neuronal somata (figure 17) located immediately proximal to

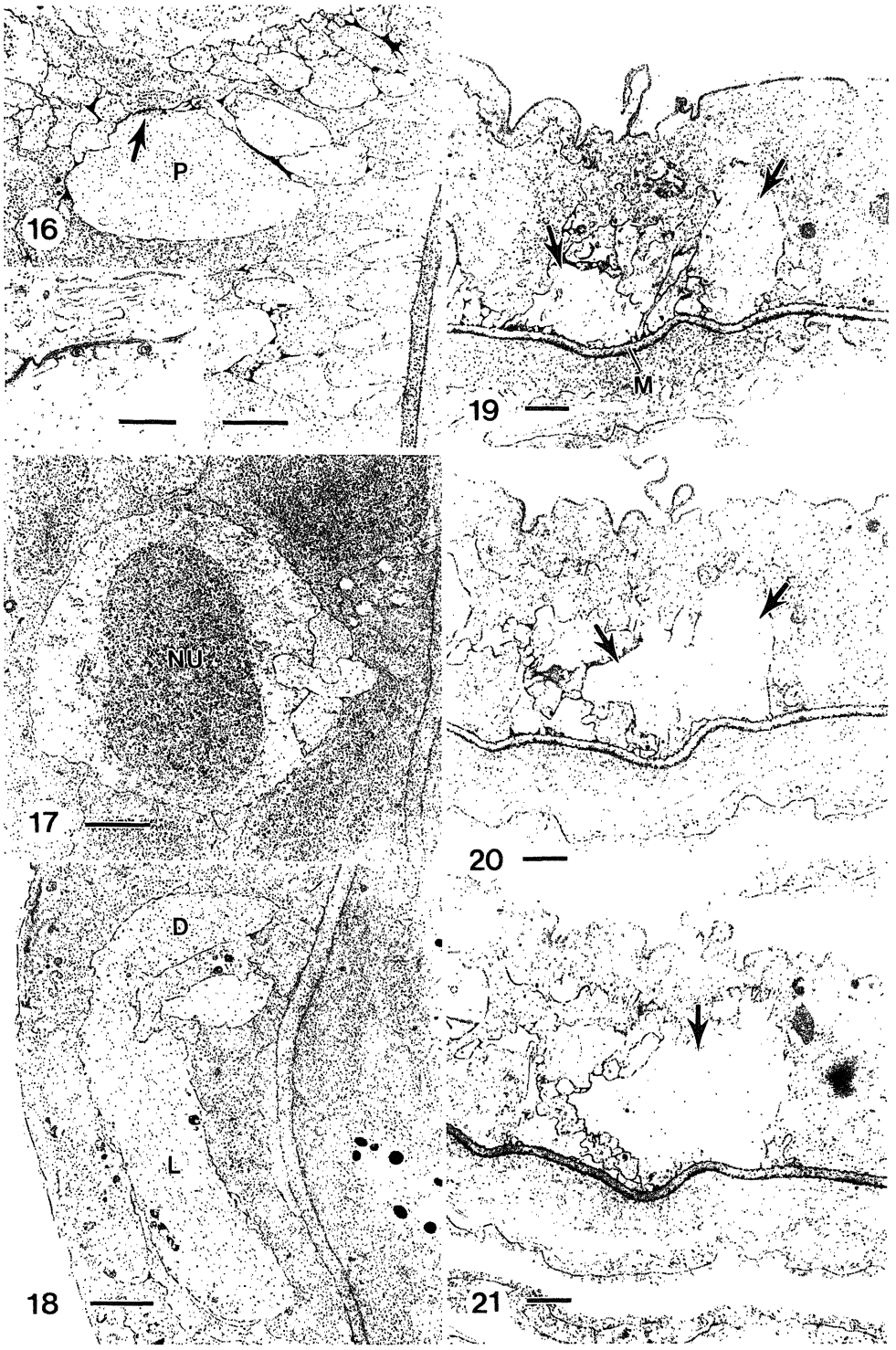

Figures 16–21. Cross sections through a giant tentacle neuron at six levels within a tentacle. See figure 15. Scale bars 2 μm.

Figure 16. Proximal neurite (P) of a giant tentacle neuron midway along tentacle base. Arrow indicates a neuromuscular synapse enlarged in the inset. Scale bar of inset 0.5 μm.

Figure 17. Nucleus (NU) of giant tentacle neuron.

Figure 18. Distal neurite (D) of giant tentacle neuron immediately below nuclear region with a lateral neurite (L) extending around autotomy plane.

Figure 19. Distal neurites (arrows) from two giant tentacle neurons; now resting on mesoglea (M) on aboral side of tentacle shaft.

Figure 20. Fusion of same distal neurites (arrows).

Figure 21. Single giant axon (arrow) formed by fusion of distal neurites from giant tentacle neurons.

PHILOSOPHICAL TRANSACTIONS OF THE ROYAL SOCIETY B BIOLOGICAL SCIENCES

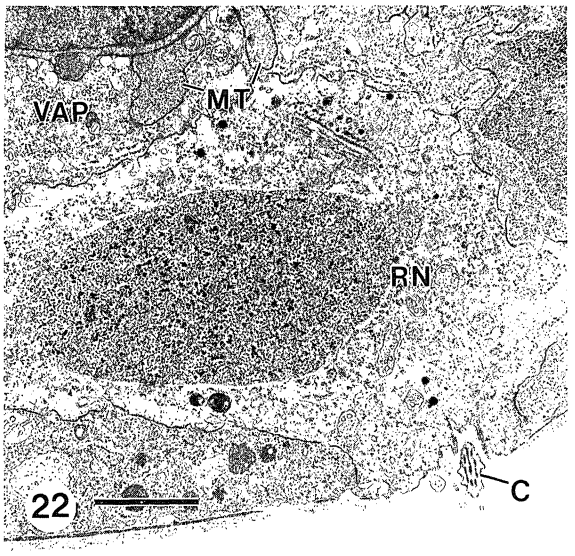

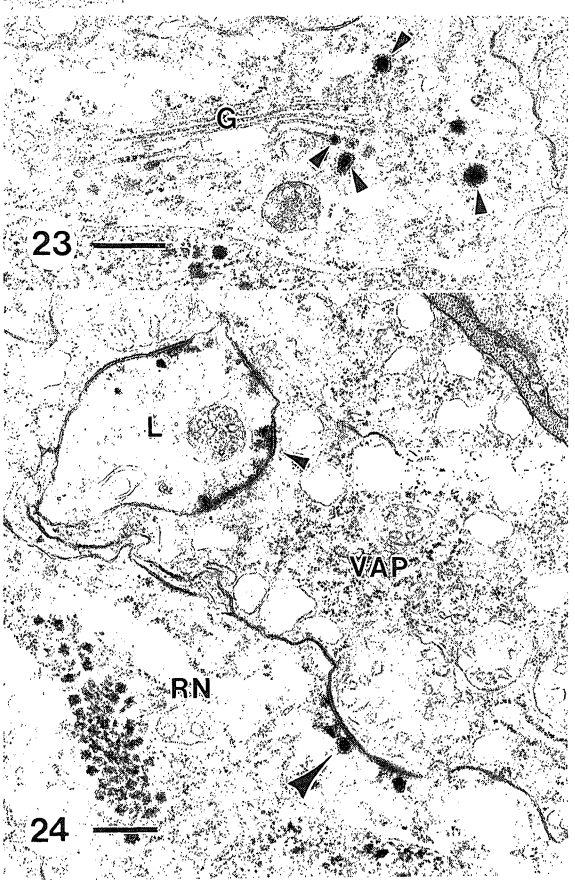

Figure 22. Cross section through oral side of tentacle autotomy plane showing nucleus and cilium (C) of a ring neuron (RN). MT, muscle tails; VAP, vacuolated autotomy plane cells. Scale bar 2 μm.
Figure 23. Golgi body (G) of a ring neuron elaborating dense-cored vesicles (arrowheads). Scale bar 0.5 μm.
Figure 24. Detail from figure 4 showing synapse (large arrowhead) of a ring neuron (RN) onto a VAP cell. Also note synapse (small arrowhead) of lateral neurite (L) of giant tentacle neuron onto the VAP cell. Scale bar 0.5 μm.

the autotomy plane. The large size and distinctive position of these giant neuronal somata allow re-identification in every tentacle, even in 1 μm sections. The somata lie too far distally along the tentacle base to be the FMRFamide-like immunoreactive 'star cells' described by Mackie *et al.* (1985). From the somata of these giant tentacle neurons, or a slight distance along their distally projecting neurites, two branches extend laterally so as to embrace the autotomy plane (figures 15 and 18). These lateral neurites, which sometimes subdivide along their trajectory around the autotomy plane (figure 9), synapse extensively with VAP cells (figures 13 and 24). The synaptic vesicles have a mean diameter of 145 nm ($n = 20$), in well-fixed tentacles (larger in poorly fixed tentacles) and contain an eccentrically placed electron-dense core surrounded by a clear halo.

In addition to proximal and lateral neurites, giant tentacle neurons each extend a distally projecting neurite. These swing aborally, come to lie directly on the mesoglea (figure 19), and just distal to the autotomy plane they fuse (figure 20) to form the previously described giant tentacle axon (Mackie 1980; Mackie & Roberts 1980; Arkett *et al.* 1988; Mackie *et al.* 1989) (figure 21). The proximally and distally projecting neurites of the giant tentacle neurons form synapses onto epitheliomuscle cells within the tentacle base and tentacle shaft, respectively (figure 16, inset).

In addition to the giant tentacle neurons, a second category of neurons, called ring neurons, is associated with the tentacle autotomy plane (figures 15 and 22). We have counted three to four somata of ring neurons per tentacle, and their laterally extended neurites collectively project around the autotomy plane within the ectoderm. In one instance, a ring neuron extended a neurite at least 50 μm proximally in the company of a giant tentacle neuron. The apical membrane of ring neurons reaches to the surface of the ectodermal epithelium and a single cilium was found occasionally at the exposed membrane (figure 22). Golgi bodies give rise to small, dense-cored vesicles (figure 23) similar to those within giant tentacle neurons. Unlike the lateral processes of giant tentacle neurons, which form many synapses onto VAP cells, we found only a few synapses between ring neurons and VAP cells (figure 24). We failed to find synapses between ring neurons and lateral neurites of giant tentacle neurons, despite the fact that the two travel adjacent to each other around much of the autotomy plane.

(iii) *Mesoglea*

Most of the mesogleal fibrils, which measure slightly less than 10 nm in diameter and have an electron-lucent core, are oriented longitudinally. These fibrils are not obviously striated in our material. Nevertheless, Muira & Kimura (1985) showed that the fine (10–30 nm) unstriated mesogleal fibrils in a scyphozoan medusa are collagenous. Electron-dense, globular elements measuring 20–30 nm are scattered among the fibrils.

With respect to density and orientation of collagen fibrils, autotomy plane mesoglea is not unusual. However, autotomy plane mesoglea is up to 50% thinner than mesoglea elsewhere along the tentacle (compare figure 4 with figures 2 and 5). The attenuation usually begins gradually, starting about 10 μm on the proximal side and up to 30 μm on the distal side of the VAP cells.

PHILOSOPHICAL TRANSACTIONS OF THE ROYAL SOCIETY B BIOLOGICAL SCIENCES

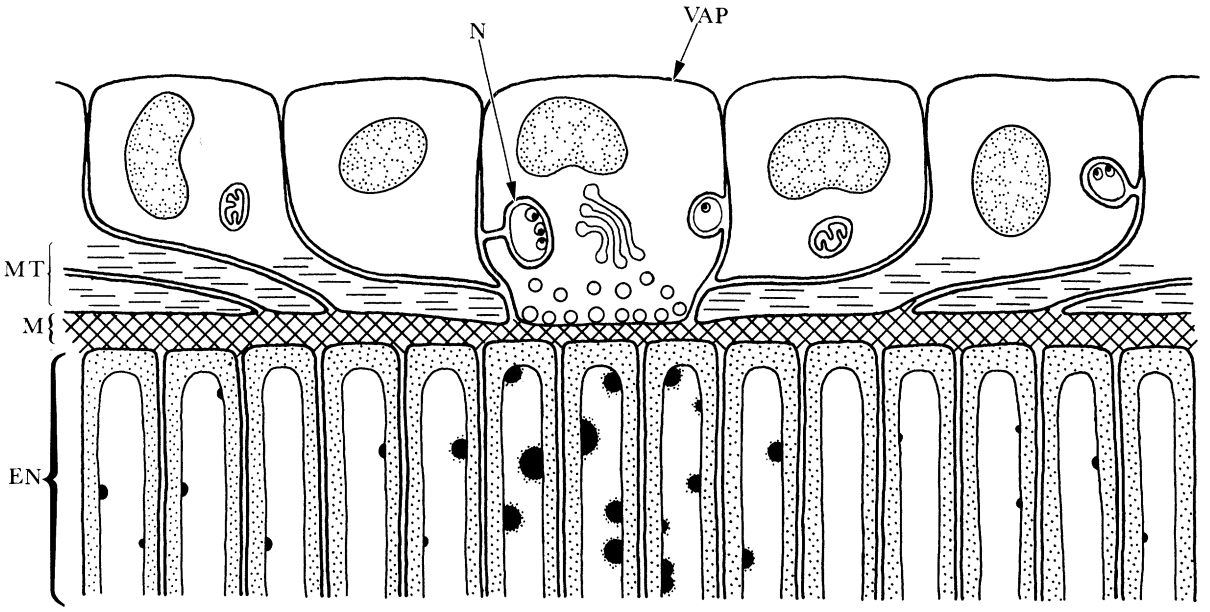

Figure 25. Diagrammatic longitudinal section through unpinched *Aglantha* tentacle. Innervated vacuolated autotomy plane cells (VAP) define the autotomy plane, interupting the sheath of muscle tails (MT) investing the tentacle (isolated slender muscle tails extending into VAP region not shown). VAP vacuoles are concentrated at basal cell membrane and the underlying mesoglea (M) is thin relative to that outside the autotomy plane. Granules within the large endodermal vacuoles are prominent within the autotomy plane. EN, endoderm; N, neurite. Drawing not to scale.

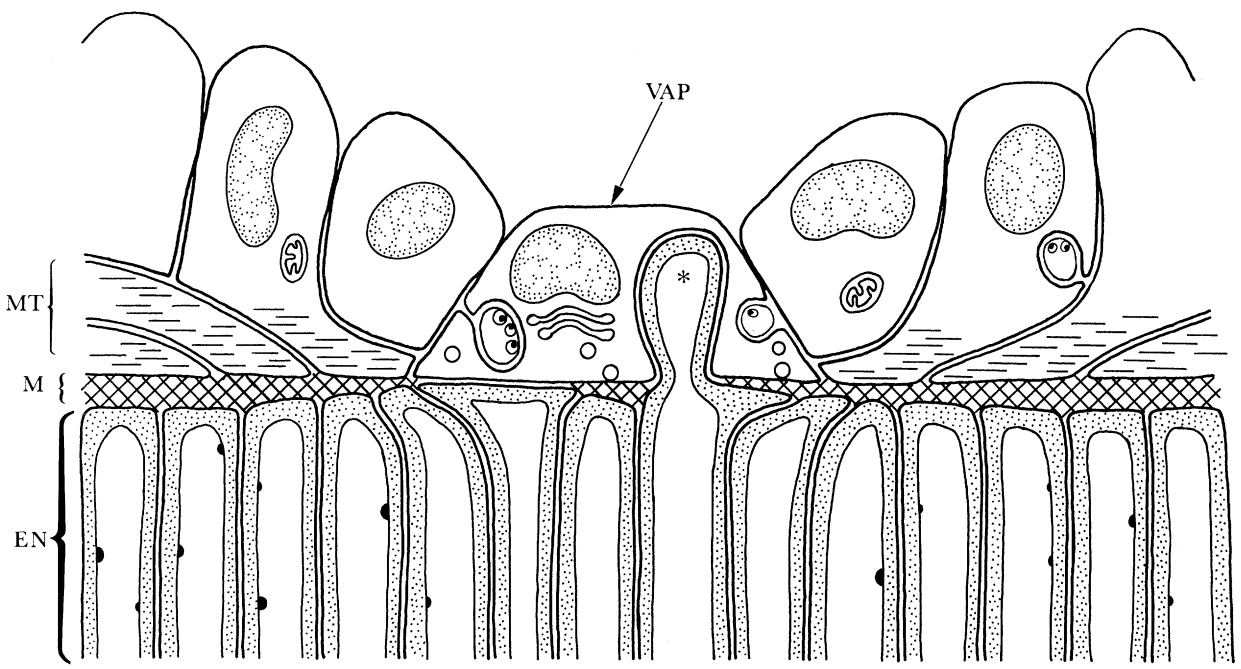

Figure 26. Diagrammatic longitudinal section through autotomy plane of pinched *Aglantha* tentacle. The mesoglea (M) has disappeared from sites beneath VAP cell and an endodermal cell has ballooned into ectoderm at one of these sites (asterisk). Other features include: loss of most vacuoles along basal VAP cell membrane, contraction of muscle tails (MT), loss of distinctive granules from endodermal vacuoles within the autotomy plane, and longitudinal extension of periphery of endodermal cells within autotomy plane. EN, endoderm. Compare with figure 25.

(iv) *Endoderm*

The gastrovascular cavity does not extend into the tentacles. The endoderm consists of a single row of cells, each containing a large vacuole. The nucleus is eccentrically placed within the rind of peripheral cytoplasm or suspended in a column of cytoplasm positioned centrally within the cell. The peripheral cytoplasm adjacent to the mesoglea is filled with microfilaments having a circular orientation. In whole mounts, endodermal cells within the tentacle shaft and whip are square or rectangular in outline, whereas those within the base are much flattened (figure 1).

The large vacuole of endodermal cells is mostly occupied by a very diffuse flocculence, often including

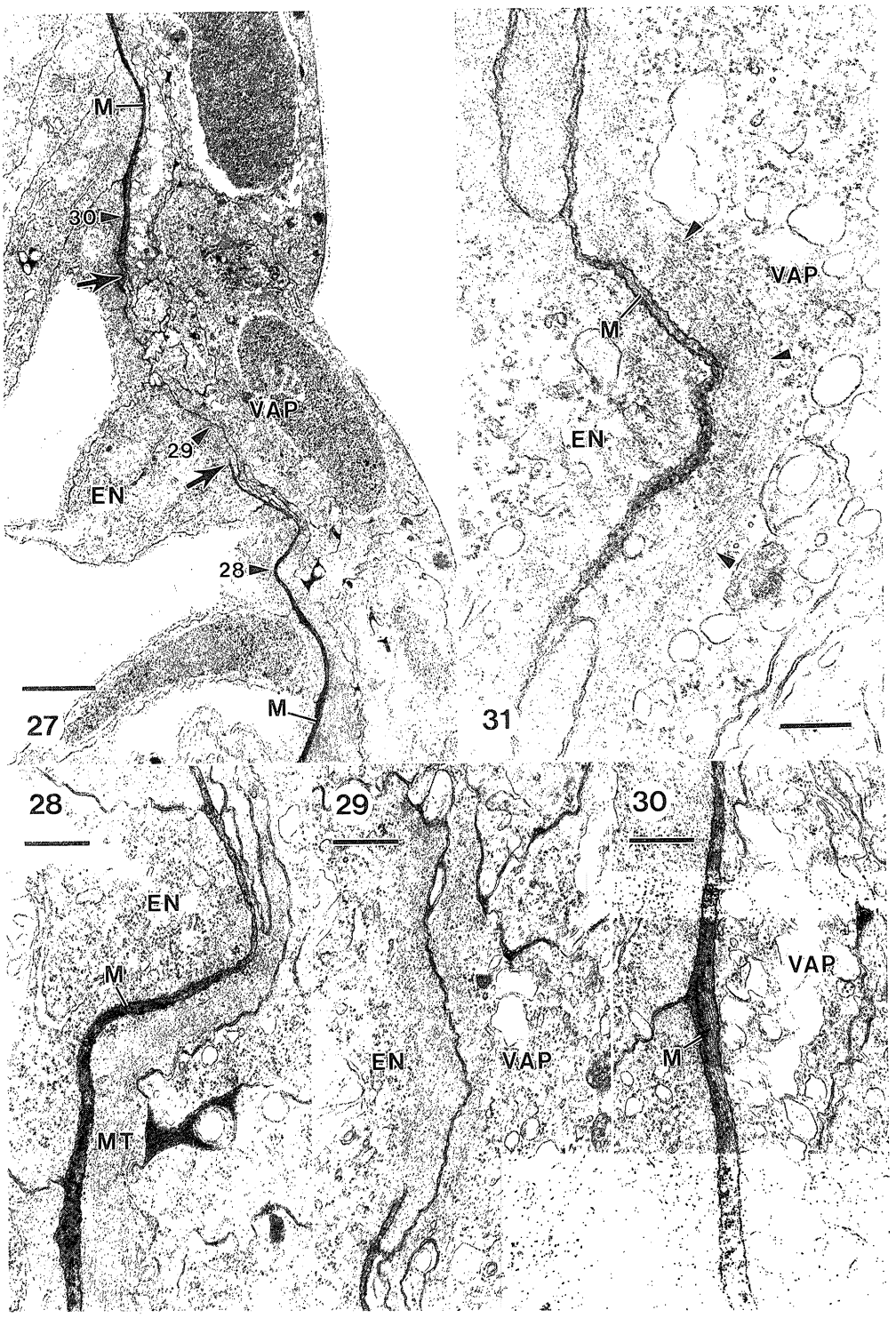

Figure 27. Longitudinal section through autotomy plane of pinched intact tentacle showing large hole in mesoglea (M; edges of hole marked by arrows) underlying vacuolated autotomy plane cell (VAP). Also note peripheral longitudinal extension of endoderm cells adjacent to mesogleal hole. Enlargements of regions indicated by numbered arrowheads are shown in figures 28, 29 and 30, respectively. Scale bar 2 μm.

Figure 28. Mesoglea (M) underlying a muscle tail (MT) on distal side of mesogleal hole. EN, endoderm. Scale bar 0.5 μm.

Figure 29. Endodermal cell (EN) juxtaposed to VAP cell with no intervening mesoglea. Note absence of vacuoles along basal membrane of VAP cell. Scale bar 0.5 μm.

Figure 30. Mesoglea (M) just proximal to the mesogleal hole with overlying VAP cell containing vacuoles adjacent to the basal membrane bordering the mesoglea. Scale bar 0.5 μm.

Figure 31. Thin, although still intact, area of mesoglea (M) within autotomy plane of a pinched intact tentacle. A feltwork of microtubules and microfilaments (arrowheads), rather than vacuoles borders the basal membrane of overlying VAP cell. EN, endoderm. Scale bar 0.3 μm.

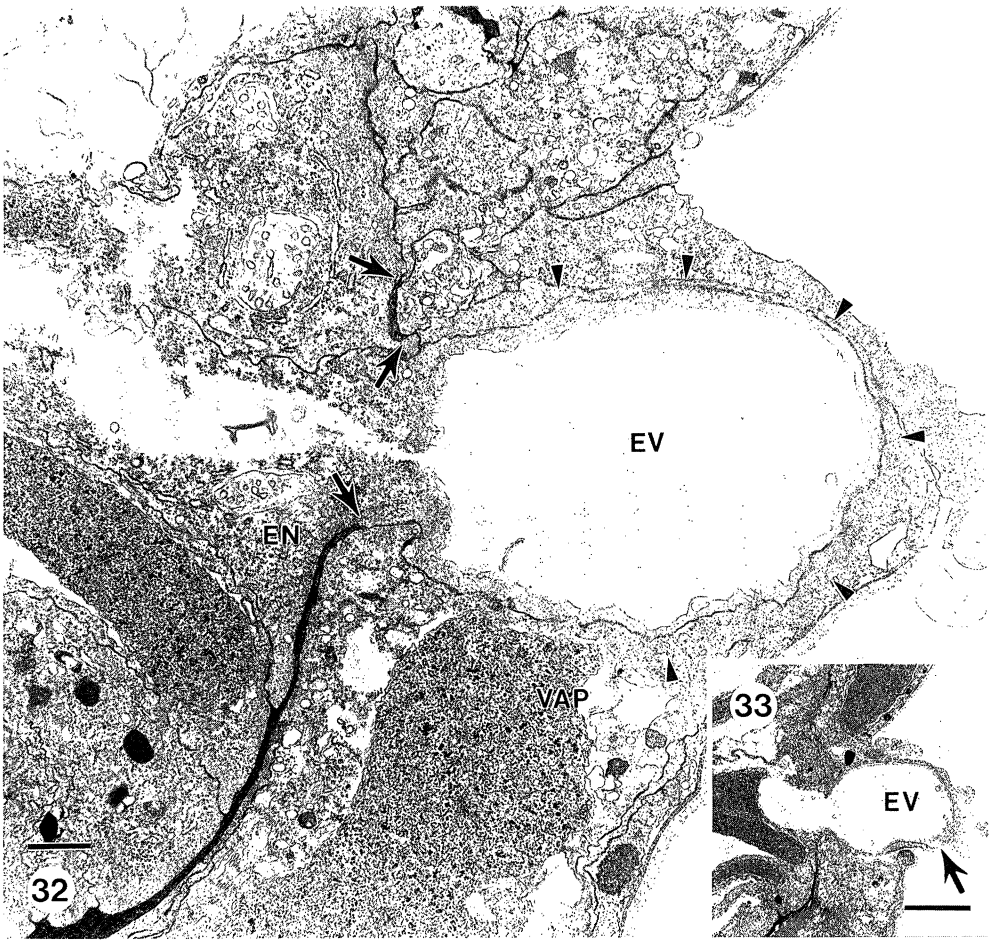

Figure 32. Longitudinal section of autotomy plane from a pinched intact tentacle showing where the cytoplasmic rind of an endodermal cell (EN), along with its central vacuole (EV) has punched through a hole in the mesoglea (broken edges of mesoglea indicated by arrows) into the overlying VAP cell. There are no vacuoles within the thin layer of VAP cell cytoplasm (arrowheads) overlying the endodermal outpocketing. Scale bar 1 μm.
Figure 33. Same area as figure 32 taken from a subsequent section. The outpocketed endodermal vacuole (EV) has broken through the overlying ectoderm at site marked by the arrow. Scale bar 5 μm.

occasional small 'membranous elements' and myelin figures. In addition, globular, electron-dense condensations may be present adjacent to the limiting membrane of the vacuole, particularly in the tentacle base. However, these condensations are always larger and more abundant within the autotomy plane (figure 9) than elsewhere along the tentacle.

General features of the autotomy plane region in unpinched tentacles are sketched in figure 25.

(*c*) *Ultrastructure of pinched intact tentacles*

We examined nine tentacles that were pinched in normal seawater but which retained an intact autotomy plane during subsequent anaesthesia and fixation. The autotomy plane of most looked much like that of unpinched tentacles, but in two we found marked changes. These changes are summarized diagrammatically in figure 26.

The most dramatic change was the presence of holes in the mesoglea of the autotomy plane (figure 27). Figures 28–30 show enlargements of three regions from figure 27. In figure 28, the mesoglea is clearly present beneath a muscle tail just distal to the autotomy plane. Within the autotomy plane, shown in figure 29, the basal membrane of the VAP cell of the ectoderm rests directly on endodermal cell membrane, except for a conventional intercellular space. Figure 29 also shows that the VAP cell overlying the mesogleal hole lacks the row of vacuoles immediately adjacent to the basal cell membrane that is so typical of VAP cells in unpinched tentacles (compare figure 29 with figures 9, 10 and 14). However, slightly more proximally in this section, a portion of VAP cell cytoplasm occurs that still has vacuoles adjacent to its basal membrane and the underlying mesoglea is intact (figure 30). In many areas where autotomy plane mesoglea is not actually ruptured, it may show marked attenuation (figure 31) compared with mesoglea within the autotomy plane of unpinched tentacles. These areas also show an absence of VAP vacuoles adjacent to the mesoglea, although vacuoles may remain in other parts of the cytoplasm. VAP cells overlying areas of mesogleal breaks or very thin mesoglea contain a zone of longitudinally aligned microtubules and microfilaments adjacent to the basal membrane (figure 31).

In one case we found that a peripheral portion of an endodermal cell had ballooned through a mesogleal

Figure 34. (*a*) LTP recorded in seawater, showing nervous pre-pulse (arrow) and epithelial after-depolarization. Asterisk shows shock. (*b*) Similar record of spontaneous STP. (*c*) LTP and STP evoked sequentially by a single shock in 130 mM Mg^{2+}. Note conduction velocity difference. (*d*) STPs in spontaneous low frequency burst, extracellular record (above), intracellular below. (*e*) LTPs (L) and STP (S) evoked by shocks. Intracellular record from epithelial cells shows depolarizations accompanying both events. Scales: (*a*) 200 μV, 20 ms; (*b*) 500 μV, 20 ms; (*c*) 200 μV, 10 ms; (*d*) 100 μV (top), 10 mV (bottom), 500 ms; (*e*) 100 μV (top), 10 mV (bottom), 50 ms.

hole into the overlying VAP cell of the autotomy plane ectoderm (figure 32). Only a thin layer of non-vacuolated VAP cell cytoplasm covered this endodermal evagination and at one point the endodermal central vacuole actually ruptured through to the exterior (figure 33).

Two types of change are seen in the endoderm within the autotomy plane of pinched tentacles. Firstly, most pinched tentacles, regardless of the appearance of mesogleal holes, show loss of the distinctive autotomy plane granules within the large endodermal vacuoles (compare figures 27 and 9). Secondly, in specimens showing mesogleal holes, the circumferential membrane of endodermal cells underlying VAP cells appears stretched out along the overlying ectoderm in both longitudinal directions (figure 27; compare with figure 9).

Examination of sections cut from the tentacle base after tentacle autotomy revealed little about the autotomy mechanism.

(*d*) *Electrophysiology*

Earlier studies (Mackie 1980; Mackie *et al.* 1989) have shown that there are two through-conduction systems in the tentacle. The faster (large tentacle pulse, LTP) system conducts at 0.6–0.9 m s^{-1} and the slower (small tentacle pulse, STP) system conducts at 0.15–0.20 m s^{-1}. The structural component responsible for LTPs is assumed to be the giant axon that runs along the aboral side of the tentacle shaft and whip, whereas STPs are assumed to be conducted in the network of smaller neurons that run throughout the tentacle. It has not been possible to record intracellularly from either neuronal component.

When recording with extracellular suction electrodes in seawater both LTPs and STPs are seen as composite events (figure 34*a*, *b*), consisting of an initial spikey component, presumably the nerve impulse (arrow), followed by a slower depolarization of variable amplitude, which is abolished in 130 mM Mg^{2+} (figure 34*c*). These secondary, variable events are recordable with microelectrodes inserted into the ectodermal epithelium (figure 34*d*, *e*) and therefore represent depolarizations of the epitheliomuscle cells. They arise from a resting potential of 60–65 mV negative. The extracellular signal presumably represents spatially summed depolarizations of many epithelial cells under the electrode tip. They are associated primarily with muscle contractions but ciliary arrests accompany contractions, and depolarizations of the ciliated cells presumably contribute to the extracellularly recorded signal.

Although the LTP system fires only once or twice after stimulation and cannot be excited without a sharp pinch or strong electric shock, the STP system

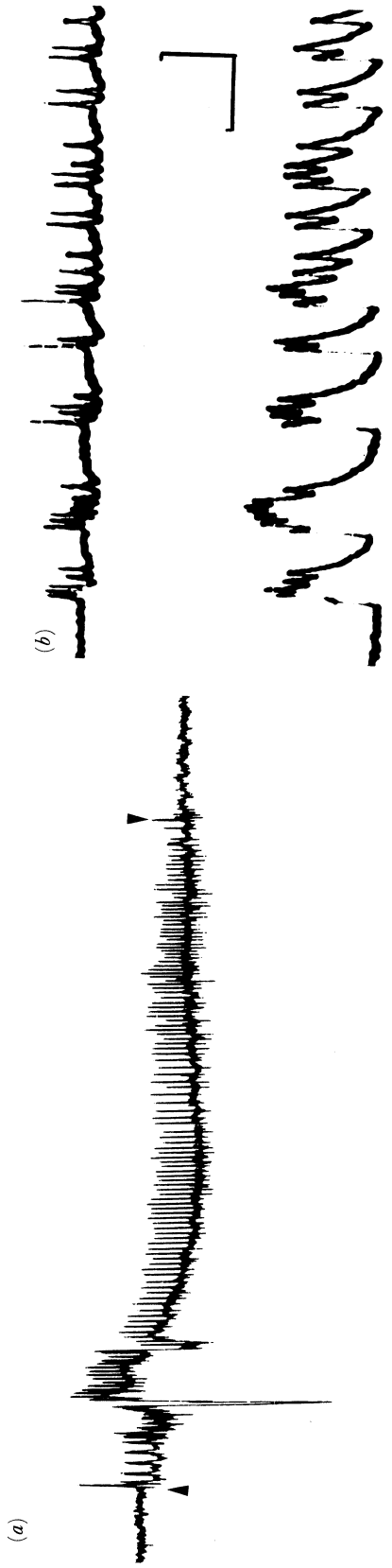

Figure 35. (*a*) Long STP burst recorded extracellularly (on chart recorder) from the base of a tentacle during autotomy. At the arrow pointing up, the tentacle was pinched. The tentacle detached at the arrow pointing down. Irregularities near start of this record are electrical artefacts caused by contortion of tentacle under the electrode. (*b*) Extracellular (above) and intracellular (below) recordings of STP burst during autotomy, showing summing depolarizations of the tentacle epithelium. Scales: (*a*) 200 μV, 400 ms; (*b*) 200 μV (top), 10 mV (bottom), 500 ms.

fires in bursts, and requires less intense stimulation. Activity in both systems travels throughout the tentacle from the site of stimulation. The STP system also fires spontaneously during normal tentacle flexion behaviour. LTP activation leads to violent tentacle contraction and (indirectly) to escape swimming (Roberts & Mackie 1980). STP activation is associated with less violent tentacle contractions, which may vary from slight coiling of the tips through intermediate steps to complete coiling up and flexion in the oral direction. The epithelial depolarizations build up gradually during a long low-frequency burst of STPs as shown by Mackie *et al.* (1989, figure 20), such bursts being associated with tentacle flexion in the oral direction.

A strong sustained pinch to the tentacle sufficient to induce autotomy is associated with a long burst of STPs at high frequency, in the range 20–40 Hz (figure 35*a*). Bursts lasting less than 2 s normally fail to produce autotomy. Such stimulation usually evokes LTP activity as well as STP, but this rarely involves more than a few impulses and it is the STP system whose sustained activity appears mainly responsible for the events culminating in autotomy. Figure 35*b* shows a portion of a typical STP burst pattern leading to autotomy. The intracellular record shows potentials summing to 15 mV peaks. The entire ectodermal epithelium appears to be depolarized during these bursts. The same pattern is recorded with a microelectrode inserted anywhere along the tentacle, including the autotomy plane.

Electrodes inserted in the vacuoles of endodermal cells (RP *ca.* 15–20 mV negative) record similar patterns to the depolarizations picked up with microelectrodes in the ectoderm and are presumably transepithelial depolarizations recorded across the outer wall of the tentacle. There is no reason to suppose that endodermal cells themselves are excited. After removal of the ectoderm, the endoderm does not conduct electrical signals or respond actively to stimulation. Electron microscopy fails to show nerves in the endoderm.

DISCUSSION

(*a*) *Autotomy mechanism*

The diameter of the tentacle at the autotomy plane is less than that of the tentacle base, yet similar to the diameter of the remainder of the tentacle. However, the autotomy plane is characterized by a thinning of mesoglea and drastic reduction in size and number of muscle tails relative to other areas of the tentacle. This provision to concentrate tensile stress in the mesoglea and muscle mass of the autotomy plane has important mechanical implications because these elements probably offer most resistance to short-term tensile stress. Muscle, particularly when contracted, resists strain along the long axis due to extensive cross-linking between myofilaments and numerous adherens junctions. Studies on passive mechanical response of anemone mesoglea have shown great extensibility of this collagenous material under low loads of long duration, but high strain resistance under short-term

loads (Chapman 1953; Alexander 1962; Gosline 1971; Koehl 1977).

Under normal conditions, thinning of autotomy plane mesoglea is tolerated without leading to ballooning of the hydrostatic skeleton through the tentacle wall because (i) the hydrostatic skeleton is partitioned into serial vacuolar compartments, allowing localization of pressure gradients along the tentacle length (see Clark 1962) and (ii) attenuation of muscle at the autotomy plane limits the pressure that can be generated within underlying endodermal vacuoles.

Structural evidence for pre-existing mechanical weakness at the tentacle autotomy plane, relative to other parts of the tentacle, is consistent with the fact that forced rupture of severely stretched tentacles anaesthetized in MgSW usually occurs at the autotomy plane.

Despite the built-in structural weakness at the tentacle autotomy plane, reversible suppression of tentacle autotomy by MgSW suggests that an active mechanism for tentacle disjunction is also involved. Although Mg^{2+} may have a direct effect on tentacle mesoglea in *Aglantha*, studies by Gosline (1971) and Koehl (1977) found no effect of this cation on passive mechanical properties of anemone mesoglea. Previous work has shown that Mg^{2+} interferes directly with muscle contraction in *Aglantha* (Kerfoot *et al.* 1985) and direct observations of autotomizing tentacles show strong, sustained contraction of the entire myoepithelium during autotomizing stimuli.

The tentacle myoepithelium is divisible into two systems that are spatially and functionally distinct. During a strong stimulus, muscle tails in the shaft and whip contract to cause tentacle retraction by coiling. The bulky muscle field extending from within the bell margin down the oral aspect of the tentacle base flexes the tentacle base toward the subumbrella. The two systems are separated by the zone of greatly reduced muscle mass at the autotomy plane. This muscle arrangement is responsible for the sphincter-like contraction seen at the autotomy plane when a strong pinch to the tentacle causes bulging of contracting myocytes on either side of the autotomy plane. There are no circular muscle tails within the tentacle.

Muscle tails projecting into the autotomy plane from the base and shaft overlap in extent, but few span the entire autotomy plane. Therefore during contraction these two muscle systems pull in opposite directions from the autotomy plane. Strong contraction of this muscle arrangement will greatly amplify tension stress at the autotomy plane during an imposed load on the tentacles.

We have described a scenario in which a zone of built-in weakness in the tentacle is subjected to further tensile stress by the arrangement and contraction of two muscle systems. This creates an apparent paradox when one considers that tentacles are regularly contracted during the swimming phase of fishing behaviour, during prey capture and transfer to the mouth, and strongly but briefly contracted during the escape swim; all without loss of tentacles. Obviously there are safety factors against inappropriate and wasteful loss of tentacles and we can identify three such factors: (i) muscle contraction must be both strong and maintained; (ii) the tentacle must be pulled by an outside agent; and (iii) VAP cells may act to weaken autotomy plane mesoglea.

The position of VAP cells, which encircle the autotomy plane, their loss of basal vacuoles that occurs concurrently with breaks in the underlying mesoglea following potentially autotomizing stimuli, and their extensive innervation argue for involvement in tentacle autotomy. Innervation of VAP cells by both giant tentacle axons and ring neurons shows them to be effectors and their ultrastructure suggests a secretory function; specifically, secretion across the basal cell membrane into the mesogleal compartment. We do not believe that VAP cells function in wound closure or healing because intact VAP cells are not recognizable at the stump of the tentacle base after autotomy. The ectodermal rim of the stump consists of epitheliomuscle cells of the tentacle base and occasional cellular fragments.

Rapid structural failure of connective tissues has been implicated in the autotomy mechanism of echinoderms (reviewed by Emson & Wilkie 1980; Wilkie 1984; Wilkie & Emson 1988) and a mollusc (see Bickell-Page 1989). In echinoderms, mechanical failure of autotomizing ligaments and tendons appears to result from weakening of matrix-mediated connections between collagen fibres. Although the mechanism may be quite different in molluscs, studied examples from both phyla show innervated granule-filled cells aligned with connective tissues subject to disjunction during autotomy, and degranulation accompanies autotomy.

VAP cells may discharge something through the basal cell membrane that reduces the tensile strength of mesoglea. Alternatively, an effect on mesogleal integrity may stem from quantitative and possibly qualitative changes to the basal cell membrane of VAP cells; massive vacuolar exocytosis must insert much vacuolar membrane into the basal membrane of VAP cells and the two types of membranes may be critically different. Weber *et al.* (1987) have demonstrated that exumbrellar ectoderm in a hydromedusa has an influence in maintaining the integrity of the underlying mesoglea attached to endoderm. After removal of ectoderm, the mesogleal fibrous system exhibits a sterotyped sequence of degradation, with the initial phase of fibre disruption occurring within minutes. *Aglantha* tentacles will autotomize within seconds during a pinch and tug but will detach much more readily if tugged after 1–2 min. of the initial pinch. If VAP cells actively participate in mesogleal rupture, then they probably provide the greatest safeguard against inappropriate tentacle autotomy.

In any event, once the mesoglea has failed, and because muscle tails spanning the autotomy plane are few and small, a weak tug should suffice to rupture both endoderm and ectoderm of the autotomy plane. The process may be aided by occasional transmesogleal extensions of muscle tails that insert on endodermal cells on either side of the autotomy plane.

In summary, strong sustained contraction of tentacle muscles evoked by a crushing pinch, in conjunction with the arrangement of muscles about the tentacle

PHILOSOPHICAL TRANSACTIONS OF THE ROYAL SOCIETY B BIOLOGICAL SCIENCES

autotomy plane and the thinning of autotomy plane mesoglea, serve to focus tensile stress at the autotomy plane when a tentacle is pulled. Existing evidence, albeit circumstantial, suggests that VAP cells also participate in autotomy, possibly to precipitate mechanical failure of stressed mesoglea at the autotomy plane. According to this interpretation, the mesoglea is the target of both active breakage mechanisms: strong, sustained muscle contraction and VAP cell activation. This is consistent with the fact that mesogleal holes appear before disjunction occurs in other autotomy plane tissues. The extreme attenuation of mesoglea immediately bordering the holes and the peripheral, longitudinal expansion of endodermal cells at the autotomy plane after potentially autotomizing stimuli suggest marked strain in autotomy plane mesoglea, compared with that of adjacent regions.

The absence of mesogleal holes in seven of the nine pinched intact tentacles we sectioned may have resulted from the fact that most tentacles in this category broke at the autotomy plane during processing for electron microscopy. Many of the pinched tentacles that remained intact during processing may have been stronger because mesogleal breakdown had not begun at the time of fixation.

A side effect of our study has been to clarify the structural relations of the tentacle giant axon. The giant axon within the shaft and whip of *Aglantha* tentacles was first recognized by Mackie (1980) and Roberts & Mackie (1980). Although the giant tentacle axon cannot be traced further proximally by light microscopy, neurophysiological results implied that it continued into the tentacle base and formed electrical synapses with the ring giant axon of the outer nerve ring (Roberts & Mackie 1980). Subsequently, preliminary observations by C. L. Singla (unpublished results cited by Arkett *et al.* (1988)) suggested that each giant tentacle axon is formed by fusion of distal processes from a pair of 'pad cells'. The expanded nuclear region of pad cells lies adjacent to mechanoreceptive comb plates (C cells) located at the base of the velum; one on either side of each tentacle. However, our results clearly show that the giant tentacle axon is the fusion product of neurites extending distally from a pair of large multipolar neurons with cell bodies located just proximal to the autotomy plane. In a future study we hope to determine if the proximal neurites of these giant tentacle neurons, which extend into the bell margin, are continuous with pad cell processes (in which case they would be multinucleate, as are the eight motor giant axons innervating the subumbrellar muscles of *Aglantha* (Weber *et al.* (1982)), or if pad cells and giant tentacle neurons are separate entities.

(*b*) *Control of autotomy: electrophysiology*

There are two conduction systems within *Aglantha* tentacles: the LTP system, characterized by fast-conducting large amplitude spikes, presumably resulting from activity in the giant tentacle neurons; and the STP system, in which smaller amplitude spikes are conducted at a slower rate relative to the LTP system. Autotomy appears to be mediated primarily by long-lasting, high-frequency bursts of activity in the STP system, which bring about summing depolarizations and strong, sustained contractions of the ectodermal muscles. Recordings from the autotomy plane show that the cells in this region depolarize like the rest of the ectoderm, so presumably the specialized vacuolated (VAP) cells in the region are also being activated, but we have no direct proof of this, as the cells penetrated were not precisely identified. Nevertheless, ring neurons that innervate VAP cells must be considered part of the STP system and gap junctions interconnect VAP cells. If VAP cells are involved in the autotomy mechanisms, their activation must depend on very high frequency impulses in the STP system, which are evoked only by crushing pinches.

The contribution of LTP activity to autotomy is probably of minor importance, but to the extent that it occurs (usually just at the start of the STP burst) it would produce EPSPs which sum with those caused by STP input. LTPs occur in all tentacles during an escape swim and are probably produced by the giant tentacle neurons, which extensively innervate VAP cells as well as epitheliomuscle cells. Assuming that VAP cells are part of the autotomy mechanism, this arrangement may be a means of priming VAP cells of all tentacles during damaging stimulation. In essence, lowering the threshold of VAP cells when probability of a direct threat to a tentacle is increased.

There is no reason to suppose that there is a special conduction system mediating the autotomy response. The response appears to reflect activity in the same systems which produce degrees of muscular contraction stopping short of autotomy. Autotomy simply requires sustained activation of the STP system at higher than normal frequency.

(*c*) *Function of autotomy*

Although tentacle autotomy may enable *Aglantha* to escape from predators, there is no evidence from field observations to support this. It seems equally likely that autotomy provides a means whereby the medusa can detach itself from prey or other objects to which its tentacles have become attached by their nematocysts. Whether the adaptation serves primarily in the context of escape from predators or from 'prey', it is the avoidance of damage which seems the most probable purpose subserved. The same applies to escape swimming in this hydromedusa. *Aglantha* live in an environment densely populated by planktonic crustaceans (Mackie & Mills 1983) including euphausiids, some far too large to be captured, but which might evoke nematocyst discharge and resulting attachment and entanglement of tentacles. Remaining attached might lead to severe damage to the medusa.

REFERENCES

Alexander, R. M. 1962 Visco-elastic properties of the body wall of sea anemones. *J. exp. Biol.* **39**, 373–386.

Arkett, S. A., Mackie, G. O. & Meech, R. W. 1988 Hair cell mechanoreception in the jellyfish *Aglantha digitale*. *J. exp. Biol.* **135**, 329–342.

PHILOSOPHICAL TRANSACTIONS OF THE ROYAL SOCIETY B BIOLOGICAL SCIENCES

Bickell-Page, L. R. 1989 Autotomy of cerata by the nudibranch *Melibe leonina* (Mollusca): ultrastructure of the autotomy plane and neural correlate of the behaviour. *Phil. Trans. R. Soc. Lond.* B **324**, 149–172.

Chapman, G. 1953 Studies on the mesoglea of coelenterates. II. Physical properties. *J. exp. Biol.* **30**, 440–451.

Clark, R. B. 1962 On the structure and function of polychaete septa. *Proc. zool. Soc. Lond.* **138**, 543–578.

Cloney, R. A. & Florey, E. 1968 Ultrastructure of cephalopod chromatophore organs. *Z. Zellforsch. mikrosk. Anat.* **89**, 73–79.

Donaldson, S., Mackie, G. O. & Roberts, A. 1980 Preliminary observations on escape swimming in *Aglantha digitale* (Hydromedusae: Trachylina). *Can. J. Zool.* **58**, 549–552.

Emson, R. H. & Wilkie, I. C. 1980 Fission and autotomy in echinoderms. *Oceanog. mar. Biol.* **18**, 155–250.

Frédéricq, L. 1883 Sur l'autotomie ou mutilation par voie réflexe comme moyen de défense chez animaux. *Arch. Zool. exp. gén.* (ser. 2) **1**, 413–426.

Gosline, J. M. 1971 Connective tissue mechanics of *Metridium senile*. II. Visco-elastic properties and macromolecular model. *J. exp. Biol.* **55**, 775–795.

Hodgson, A. N. 1984 Use of the intrinsic musculature for siphonal autotomy in the Solenacea (Mollusca). *Trans. R. Soc. S. Afr.* **45**, 129–138.

Kerfoot, P. A. H., Mackie, G. O., Meech, R. W., Roberts, A. & Singla, C. L. 1985 Neuromuscular transmission in the jellyfish *Aglantha digitale*. *J. exp. Biol.* **116**, 1–25.

Koehl, M. A. P. 1977 Mechanical diversity of connective tissue of the body wall of sea anemones. *J. exp. Biol.* **69**, 107–125.

Mackie, G. O. 1980 Slow swimming and cyclical 'fishing' behavior in *Aglantha digitale* (Hydromedusae: Trachylina). *Can. J. Fish. aquat. Sci.* **37**, 1550–1556.

Mackie, G. O. & Meech, R. W. 1985 Separate sodium and calcium spikes in the same axon. *Nature, Lond.* **313**, 791–793.

Mackie, G. O. & Mills, C. E. 1983 Use of PISCES IV submersible for zooplankton studies in coastal waters of British Columbia. *Can. J. Fish. aquat. Sci.* **40**, 763–776.

Mackie, G. O., Nielsen, C. & Singla, C. L. 1989 The tentacle cilia of *Aglantha digitale* (Hydrozoa: Trachylina) and their control. *Acta Zool., Stockholm* **70**, 133–141.

Mackie, G. O., Pugh, P. R. & Purcell, J. E. 1987 Siphonophore biology. *Adv. mar. Biol.* **24**, 97–262.

Mackie, G. O., Singla, C. L. & Stell, W. K. 1985 Distribution of nerve elements showing FMRFamide-like immunoreactivity in Hydromedusae. *Acta Zool., Stockholm* **66**, 199–210.

McVean, A. 1982 Autotomy. In *Biology of Crustacea* (ed. D. C. Sandeman & H. L. Atwood), pp. 107–132. New York: Academic Press.

Muira, S. & Kimura, S. 1985 Jellyfish mesogloea collagen. *J. biol. Chem.* **260**, 15352–15356.

Purcell, J. E. 1977 Aggressive function and induced development of catch tentacles in the sea anemone *Metridium senile* (Coelenterata, Actinaria). *Biol. Bull. mar. Biol. Lab. Woods Hole* **153**, 355–368.

Roberts, A. & Mackie, G. O. 1980 The giant axon escape system of a hydrozoan medusa, *Aglantha digitale*. *J. exp. Biol.* **84**, 303–318.

Sheppard, L. & Bellairs, Ad'A. 1972 The mechanism of autotomy in *Lacerta*. *Br. J. Herpet.* **4**, 276–286.

Singla, C. L. 1978 Locomotion and neuromuscular system in *Aglantha digitale*. *Cell Tiss. Res.* **188**, 317–327.

Stasek, C. R. 1967 Autotomy in the Mollusca. *Occ. Pap. Calif. Acad. Sci.* **61**, 1–44.

Wake, D. B. & Dresner, I. G. 1967 Functional morphology and evolution of tail autotomy in salamanders. *J. Morph.* **122**, 265–306.

Weber, C., Kurz, E. & Schmid, V. 1987 The fibrous system of the extracellular matrix of *Podocoryne carnea* and its degradation by the subumbrellar plate endoderm demonstrated by a monoclonal antibody. *Tiss. Cell* **19**, 757–771.

Weber, C., Singla, C. L. & Kerfoot, P. A. H. 1982 Microanatomy of the subumbrellar motor innervation in *Aglantha digitale* (Hydromedusae: Trachylina). *Cell Tiss. Res.* **223**, 305–312.

Wilkie, I. C. 1984 Variable tensility in echinoderm collagenous tissues: a review. *Mar. Behav. Physiol.* **11**, 1–34.

Wilkie, I. C. & Emson, R. H. 1988 Mutable collagenous tissues and their significance for echinoderm palaeontology and phylogeny. In *Echinoderm phylogeny and evolutionary biology* (ed. C. R. Paul & A. B. Smith), pp. 311–330. Oxford: Clarendon Press.

Received 2 August 1990; accepted 12 September 1990

PHILOSOPHICAL TRANSACTIONS OF THE ROYAL SOCIETY B BIOLOGICAL SCIENCES

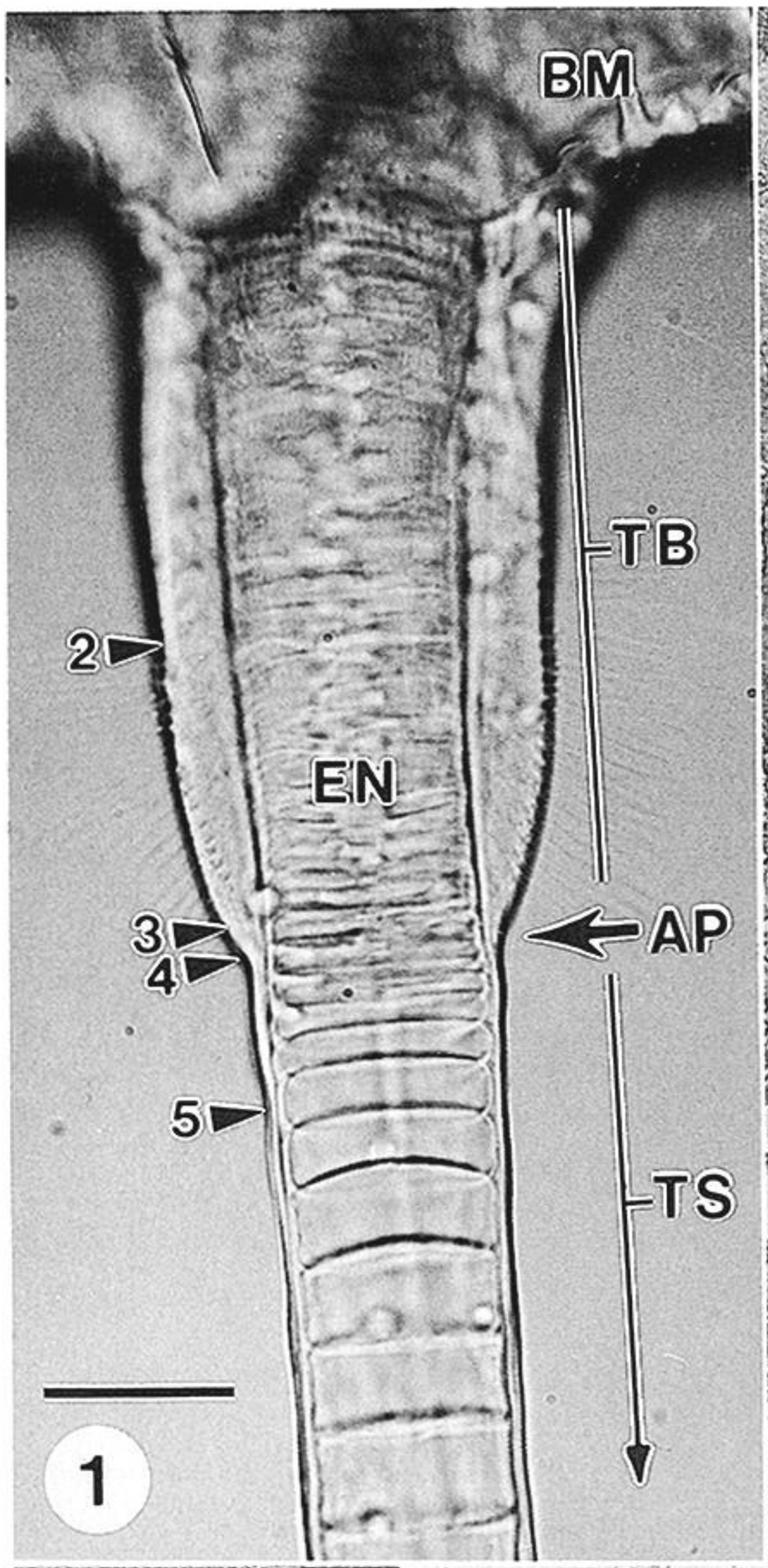

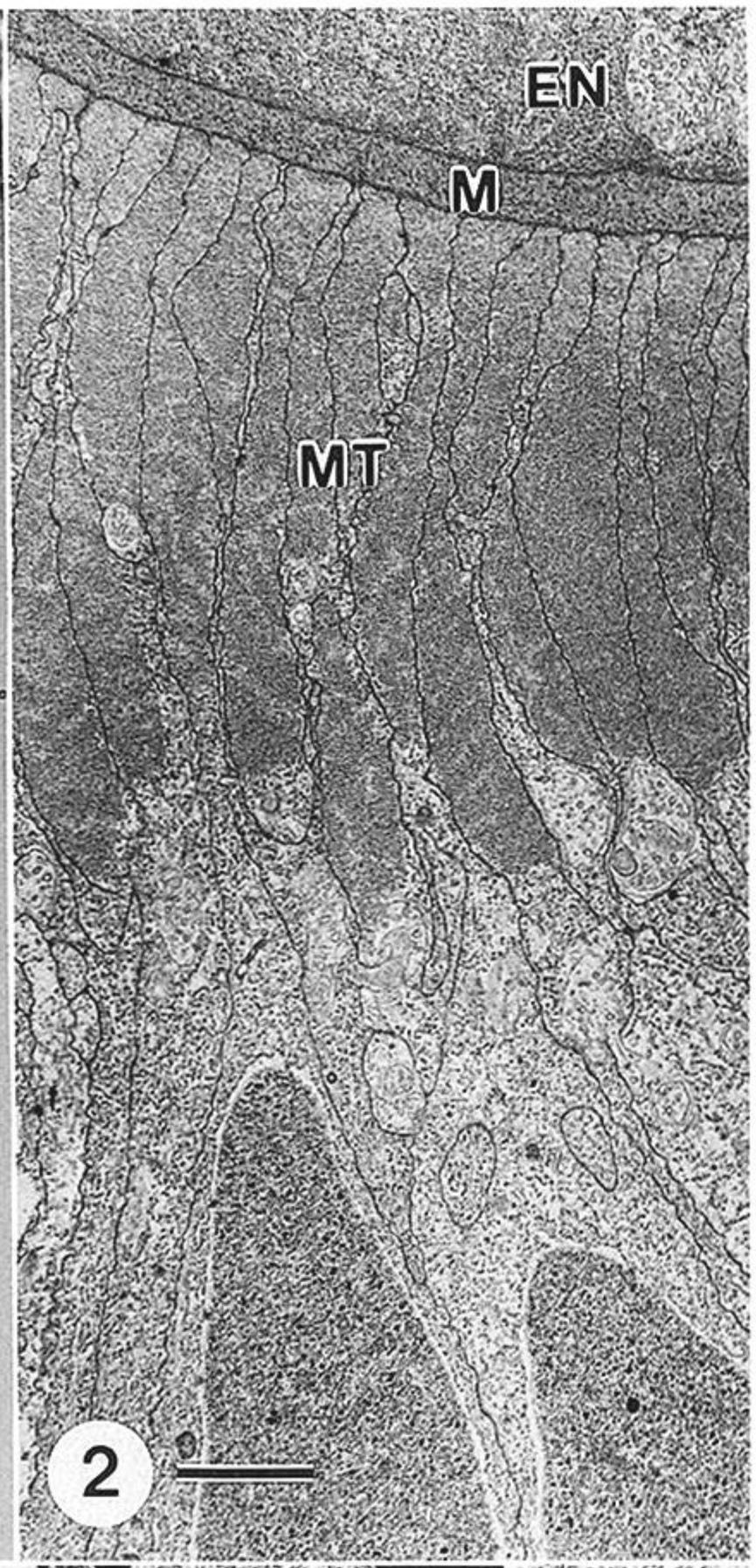

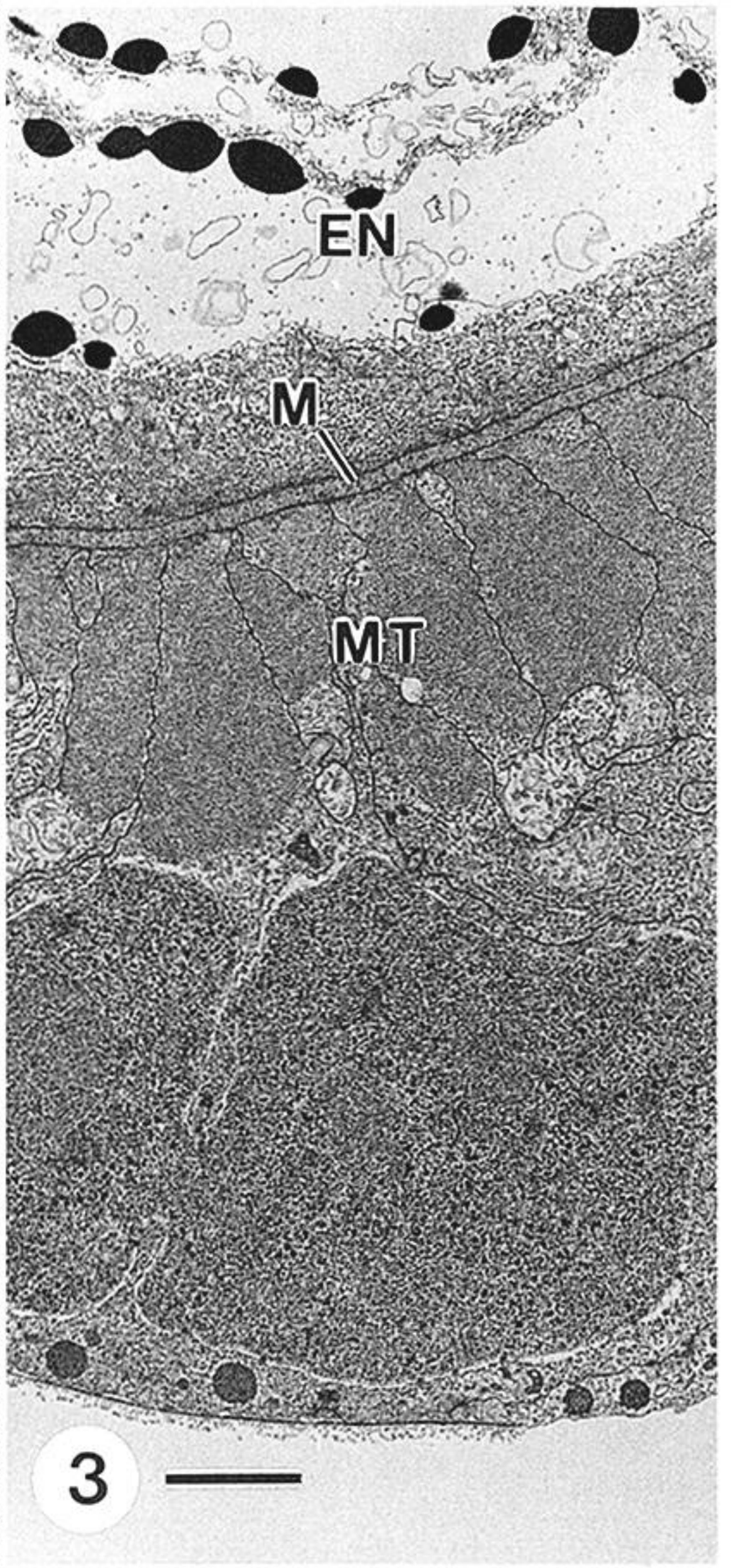

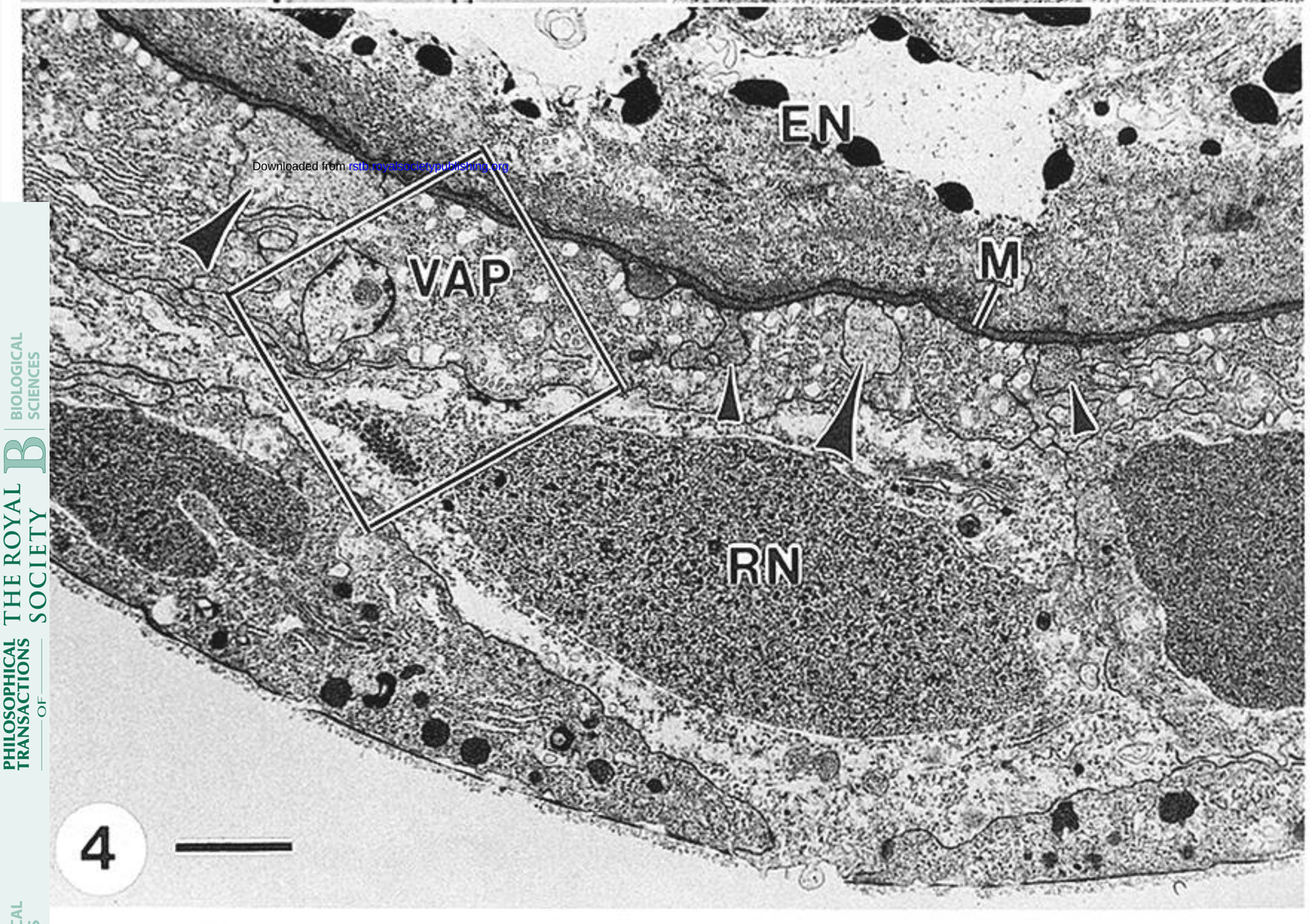

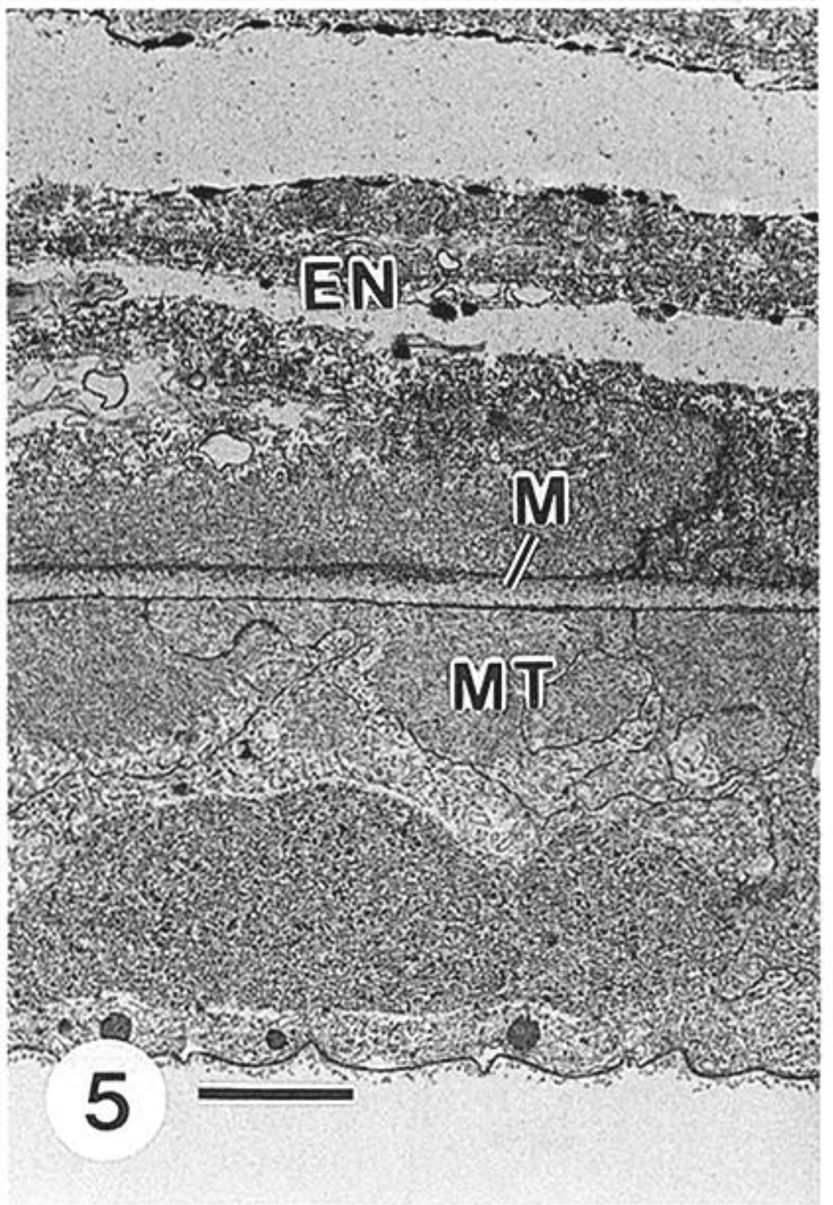

Figure 1. Photomicrograph of a tentacle base (TB) attached to the bell margin (BM), tentacle shaft (TS), and autotomy plane (AP). EN, endoderm. Numbered arrowheads indicate levels of cross sections shown in figures 2–5. Scale bar 50 μm.

Figures 2–5. Cross sections of epitheliomuscle cells on oral side of tentacle at four different levels. EN, endoderm; M, mesoglea; MT, muscle tails. Scale bars 2 μm.

Figure 2. Midway along tentacle base; muscle tails shaped as broad ribbons.

Figure 3. Extreme distal end of tentacle base.

Figure 4. Autotomy plane; vacuolated autotomy plane cells (VAP) surround small, isolated muscle tails extending from the tentacle base (small arrowheads) and from the tentacle shaft (large arrowheads). Note thin mesoglea. Boxed area enlarged in figure 24. RN, ring neuron.

Figure 5. Tentacle shaft approximately 20 μm distal to autotomy plane.

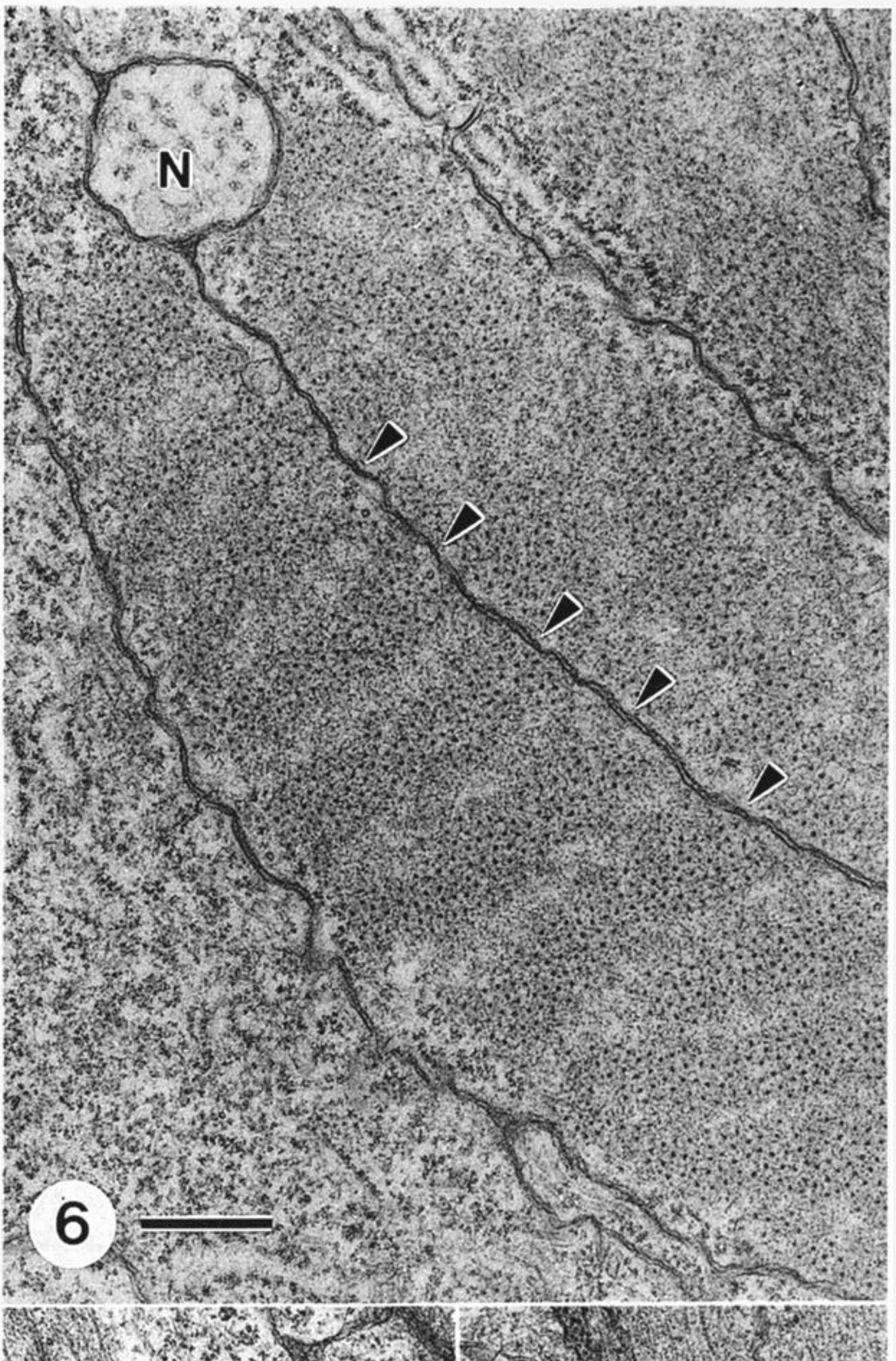

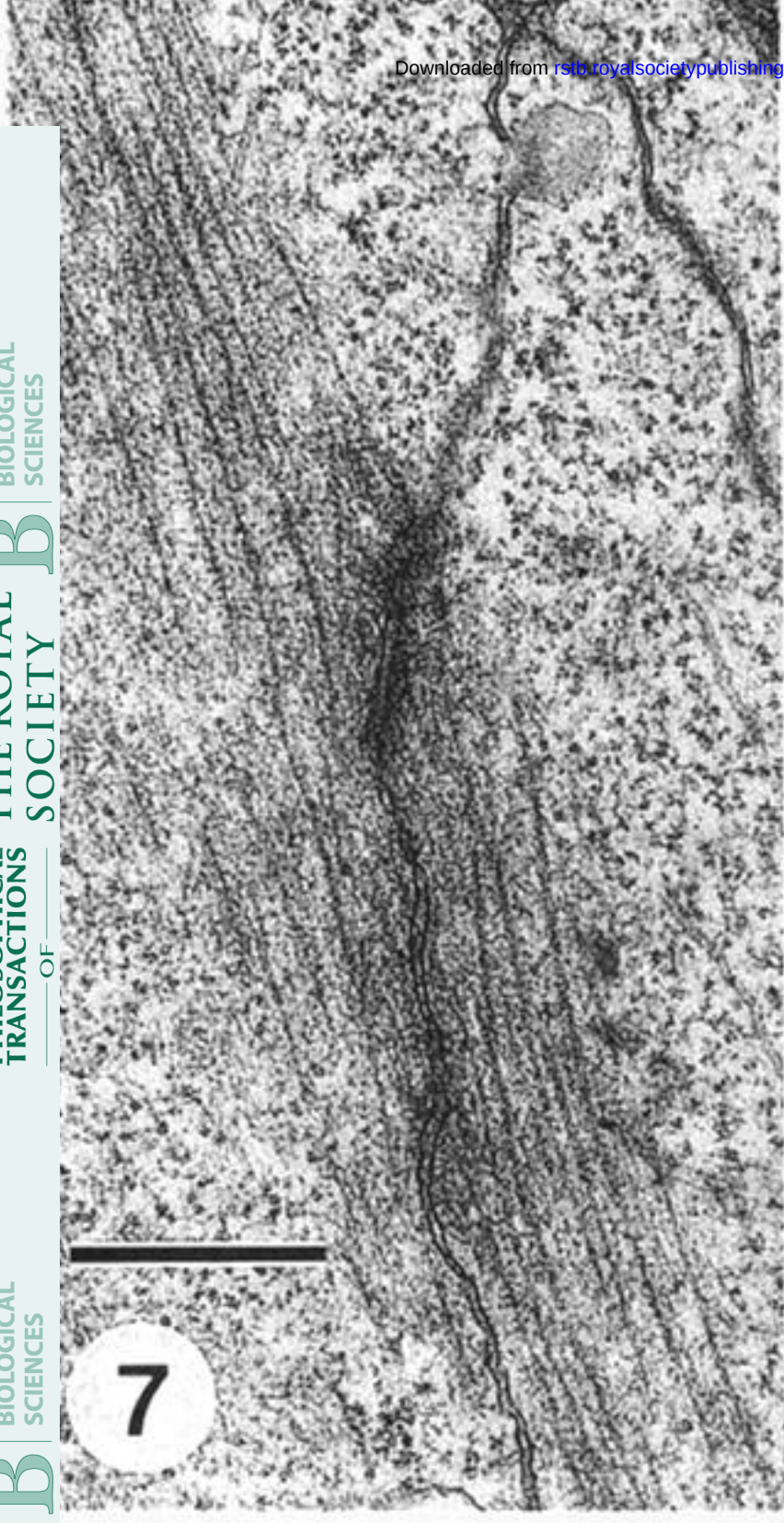

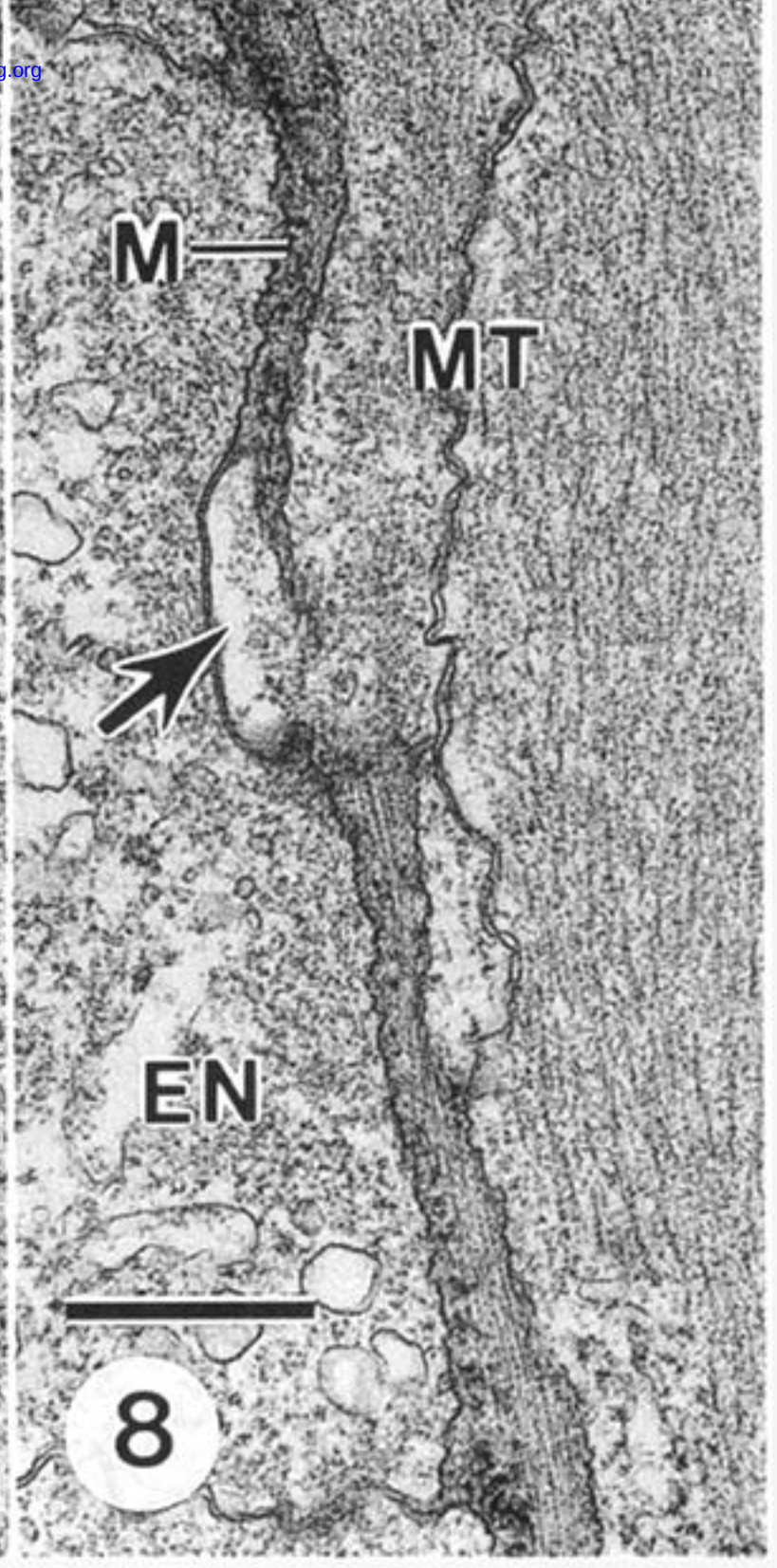

gure 6. Cross section through a muscle tail showing ternating zones of thick (arrowheads) and thin filaments. small neurite. Scale bar 0.5 μm.

gure 7. Adherens junction between adjacent muscle tails. ale bar 0.5 μm.

gure 8. Cytoplasmic process (arrow) from a muscle tail IT) extending across mesoglea (M) just distal to autotomy ane. EN, endoderm. Scale bar 0.5 μm.

gure 9. Longitudinal section through the autotomy plane on oral side of tentacle. Muscle tails (MT) from tentacle ıse abut with vacuolated autotomy plane cell (VAP) with vacuoles concentrated towards thin mesoglea (M). ction passes through two branches of a lateral neurite (L) from a giant tentacle neuron and a neurite from a ring uron (RN). CN, cnidocyte; EG, endodermal granules. Scale bar 2 μm.

gure 10. Longitudinal section showing vacuoles of VAP cells lined-up along basal membrane adjacent to mesoglea I). Scale bar 0.5 μm.

gure 11. Detail of VAP vacuoles adjacent to basal cell membrane. Scale bar 0.1 μm.

gure 12. Gap junction between VAP cells. Scale bar 0.1 μm.

gure 13. Longitudinal, tangential section through the autotomy plane showing synaptic sites (arrows) between a teral neurite (L) of a giant tentacle neuron and VAP cell. Arrowheads indicate microtubules. Scale bar 0.5 μm.

gure 14. Adherens junction (arrow) between a small muscle tail (MT) and a VAP cell. M, mesoglea. Scale bar 5 μm.

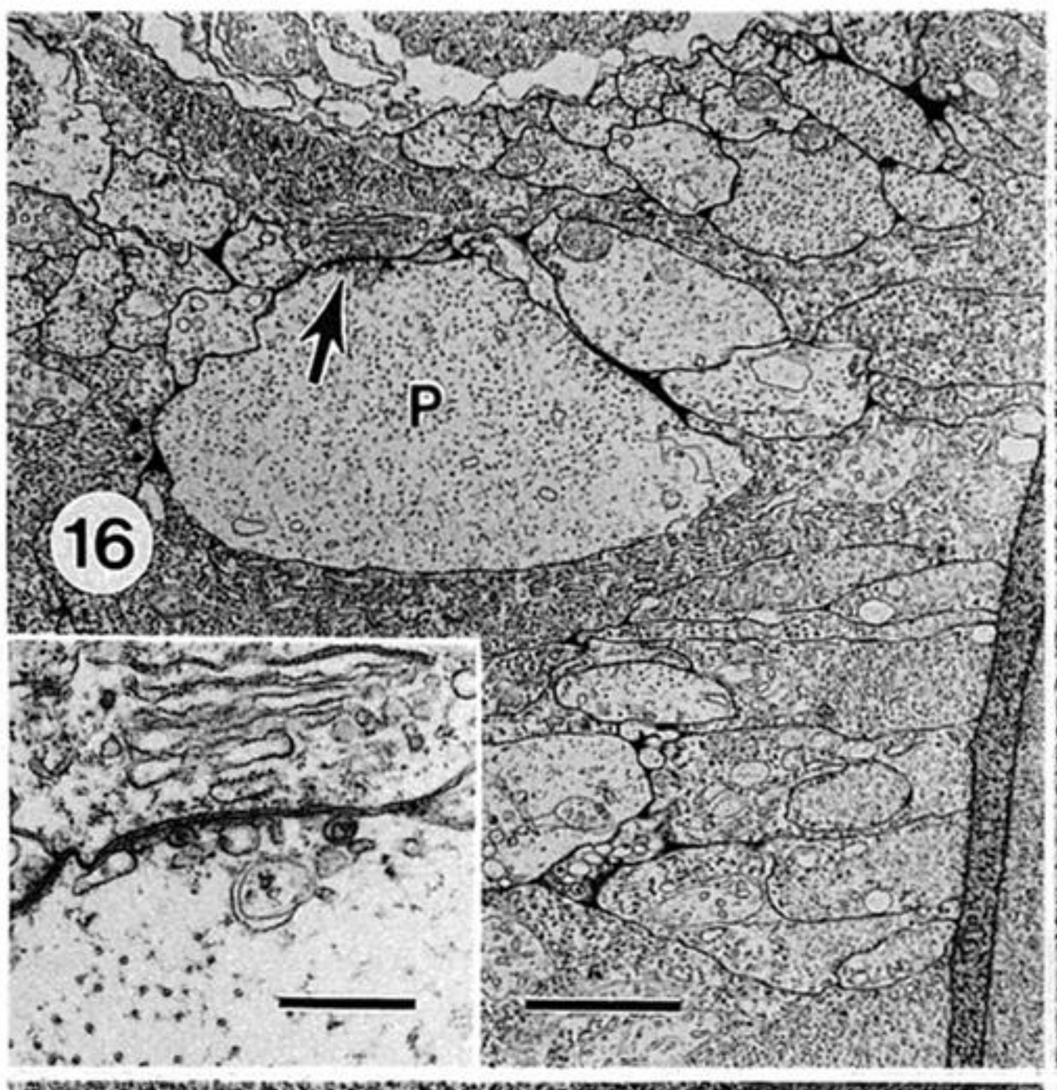

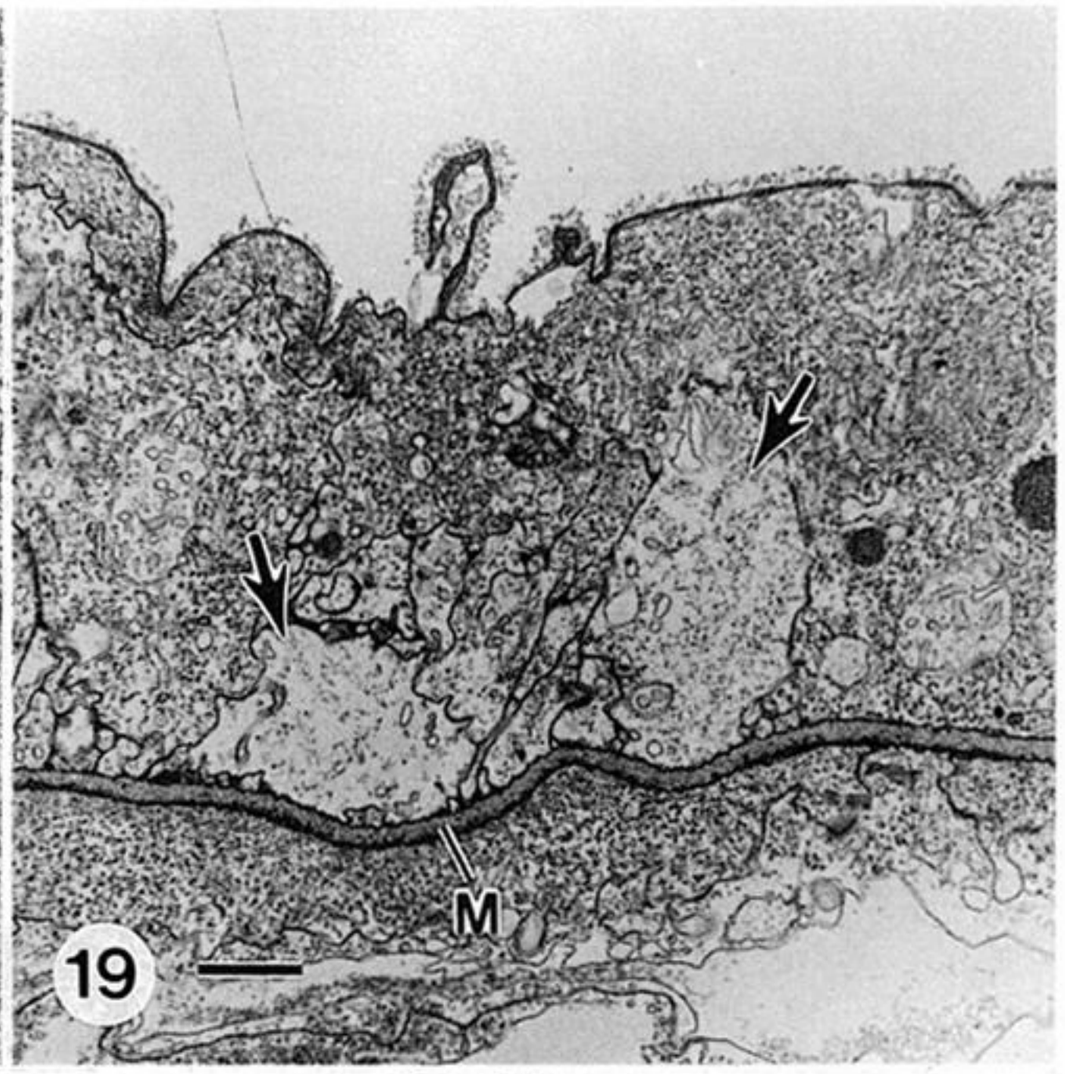

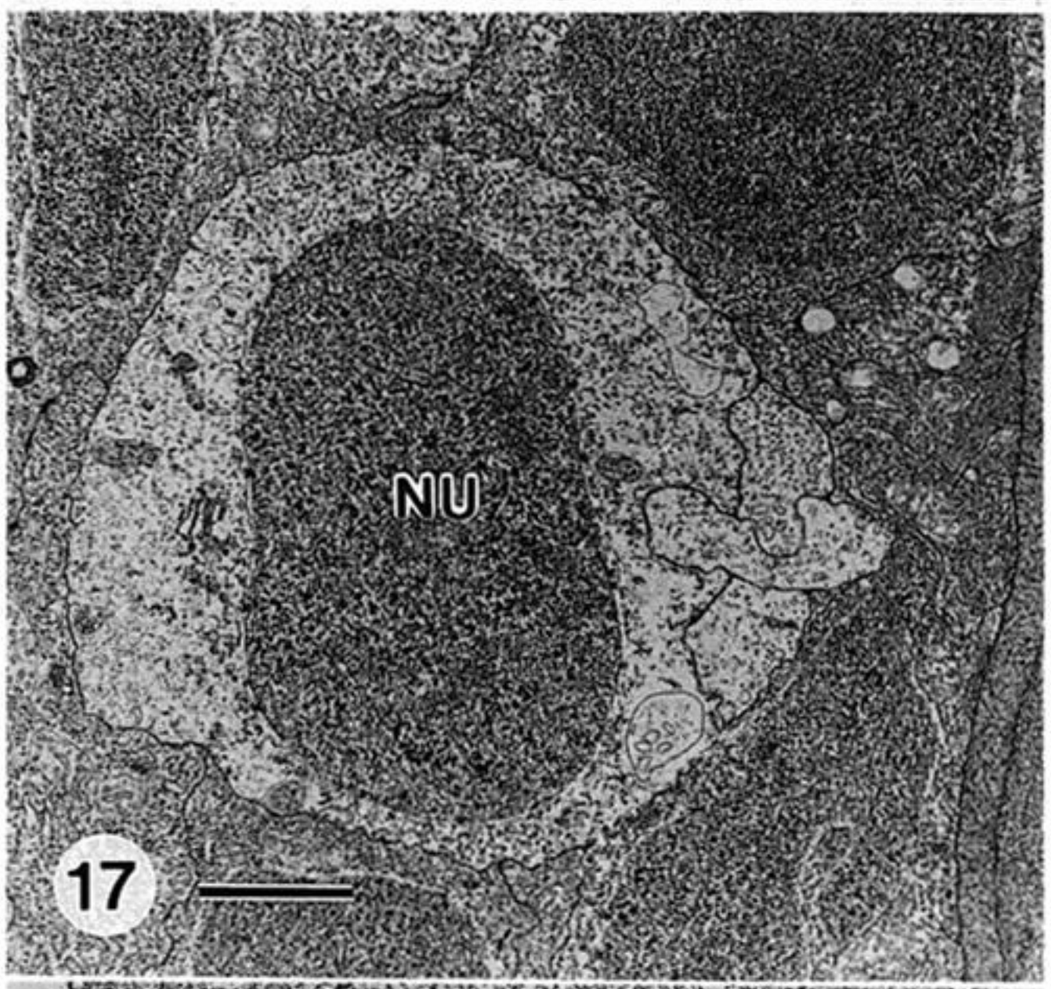

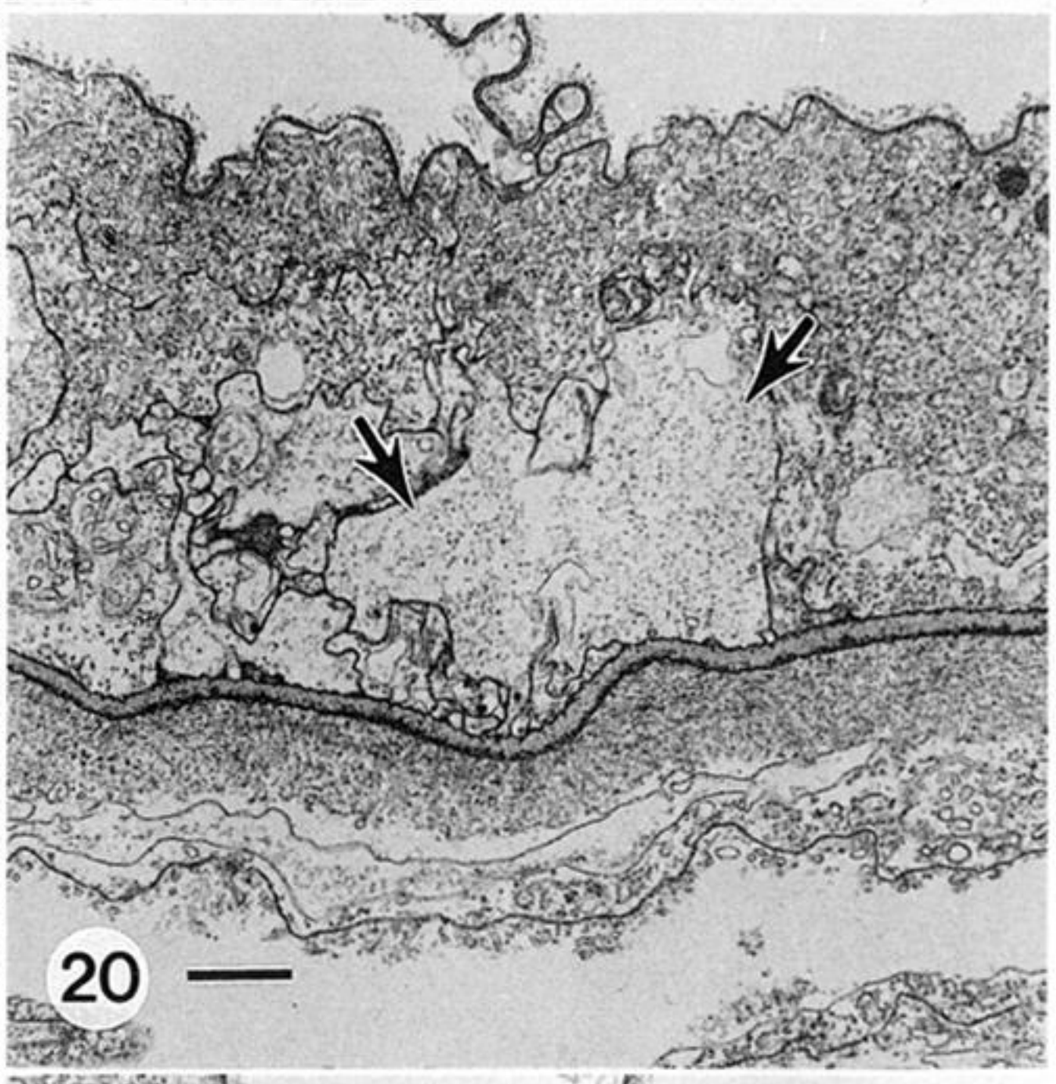

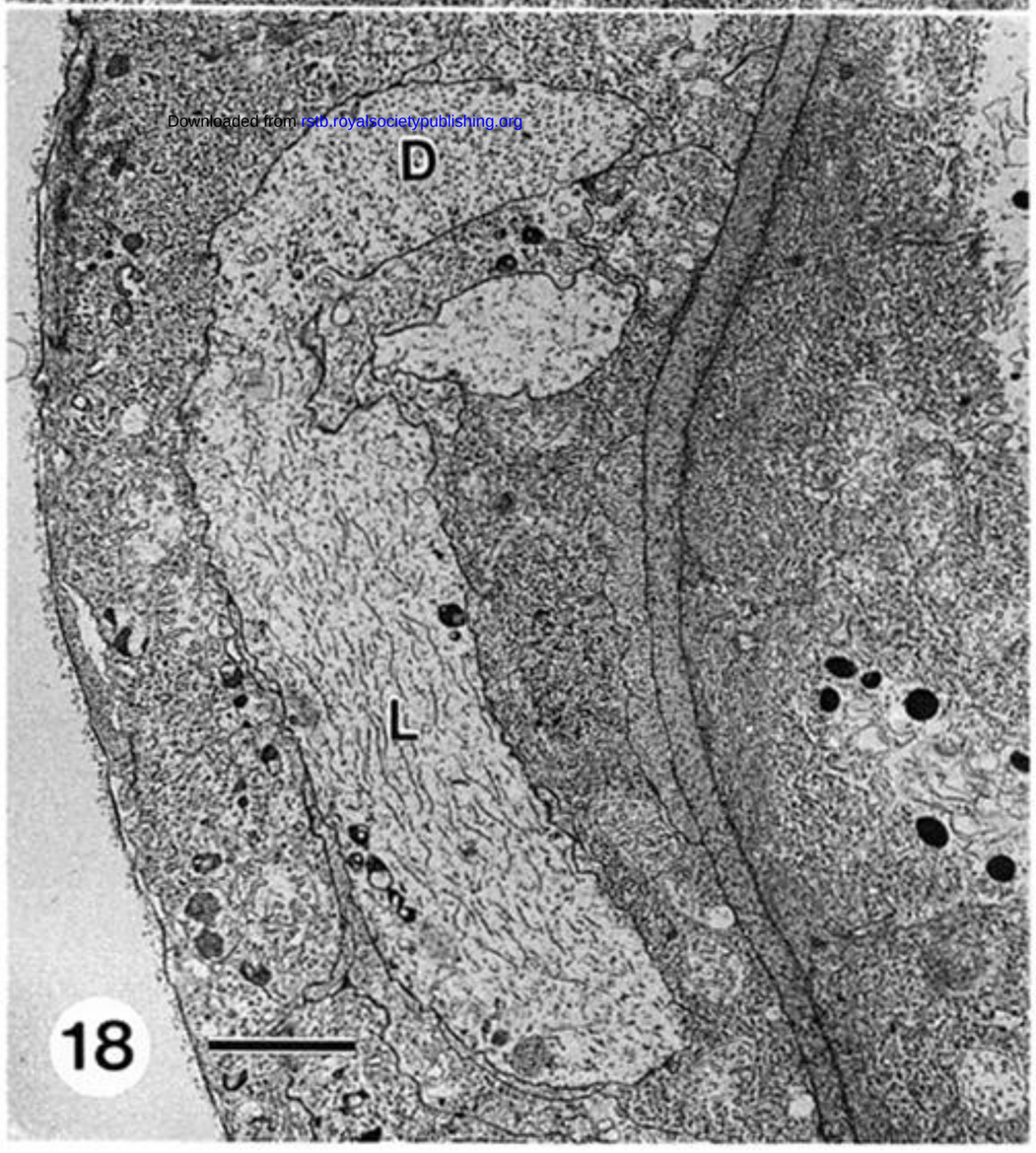

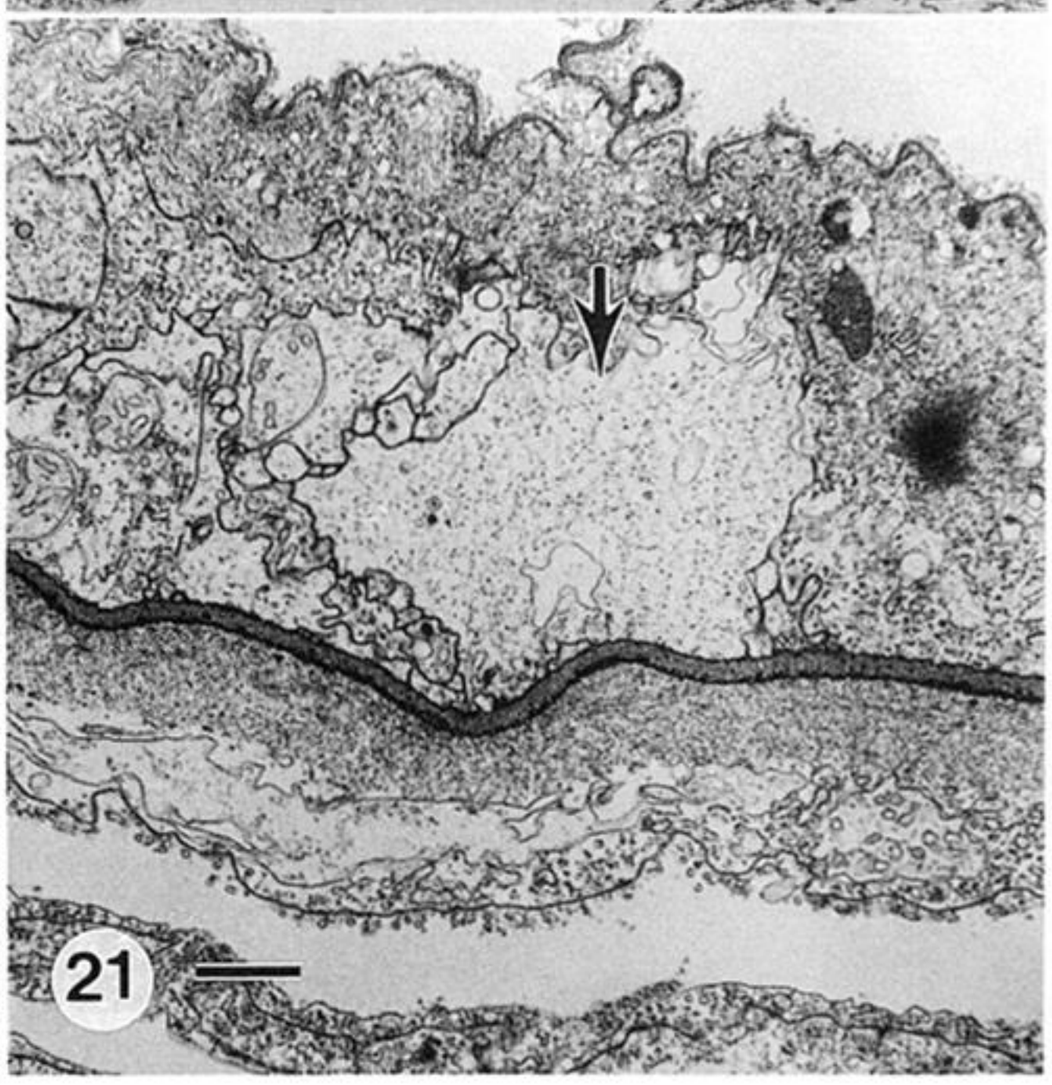

gures 16–21. Cross sections through a giant tentacle neuron at six levels within a tentacle. See figure 15. Scale bars μm.

gure 16. Proximal neurite (P) of a giant tentacle neuron midway along tentacle base. Arrow indicates a uromuscular synapse enlarged in the inset. Scale bar of inset 0.5 μm.

gure 17. Nucleus (NU) of giant tentacle neuron.

gure 18. Distal neurite (D) of giant tentacle neuron immediately below nuclear region with a lateral neurite (L) tending around autotomy plane.

gure 19. Distal neurites (arrows) from two giant tentacle neurons; now resting on mesoglea (M) on aboral side of ntacle shaft.

gure 20. Fusion of same distal neurites (arrows).

gure 21. Single giant axon (arrow) formed by fusion of distal neurites from giant tentacle neurons.

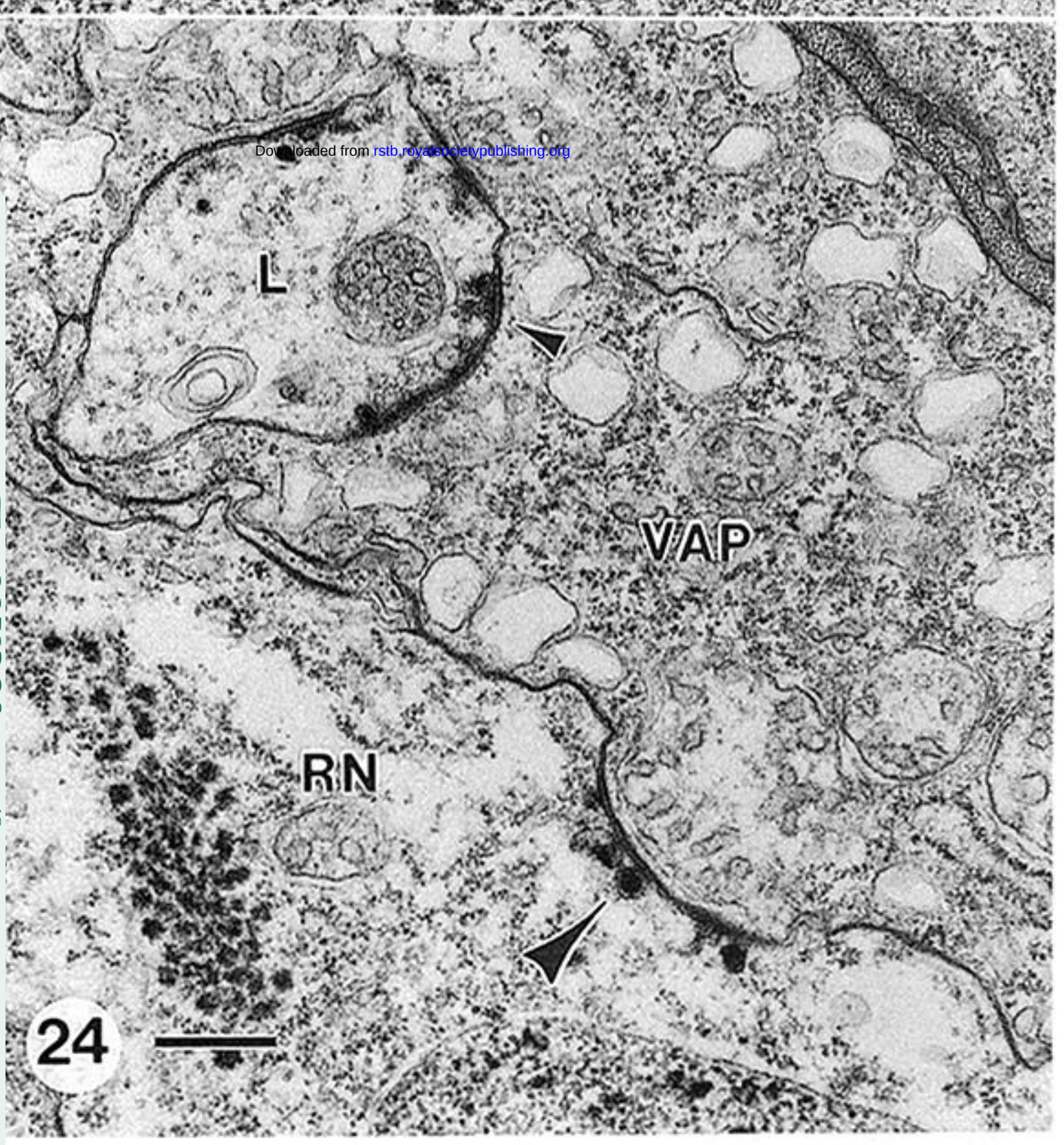

gure 22. Cross section through oral side of tentacle totomy plane showing nucleus and cilium (C) of a ring uron (RN). MT, muscle tails; VAP, vacuolated autotomy ane cells. Scale bar 2 μm.

gure 23. Golgi body (G) of a ring neuron elaborating nse-cored vesicles (arrowheads). Scale bar 0.5 μm.

gure 24. Detail from figure 4 showing synapse (large rowhead) of a ring neuron (RN) onto a VAP cell. Also note napse (small arrowhead) of lateral neurite (L) of giant ntacle neuron onto the VAP cell. Scale bar 0.5 μm.

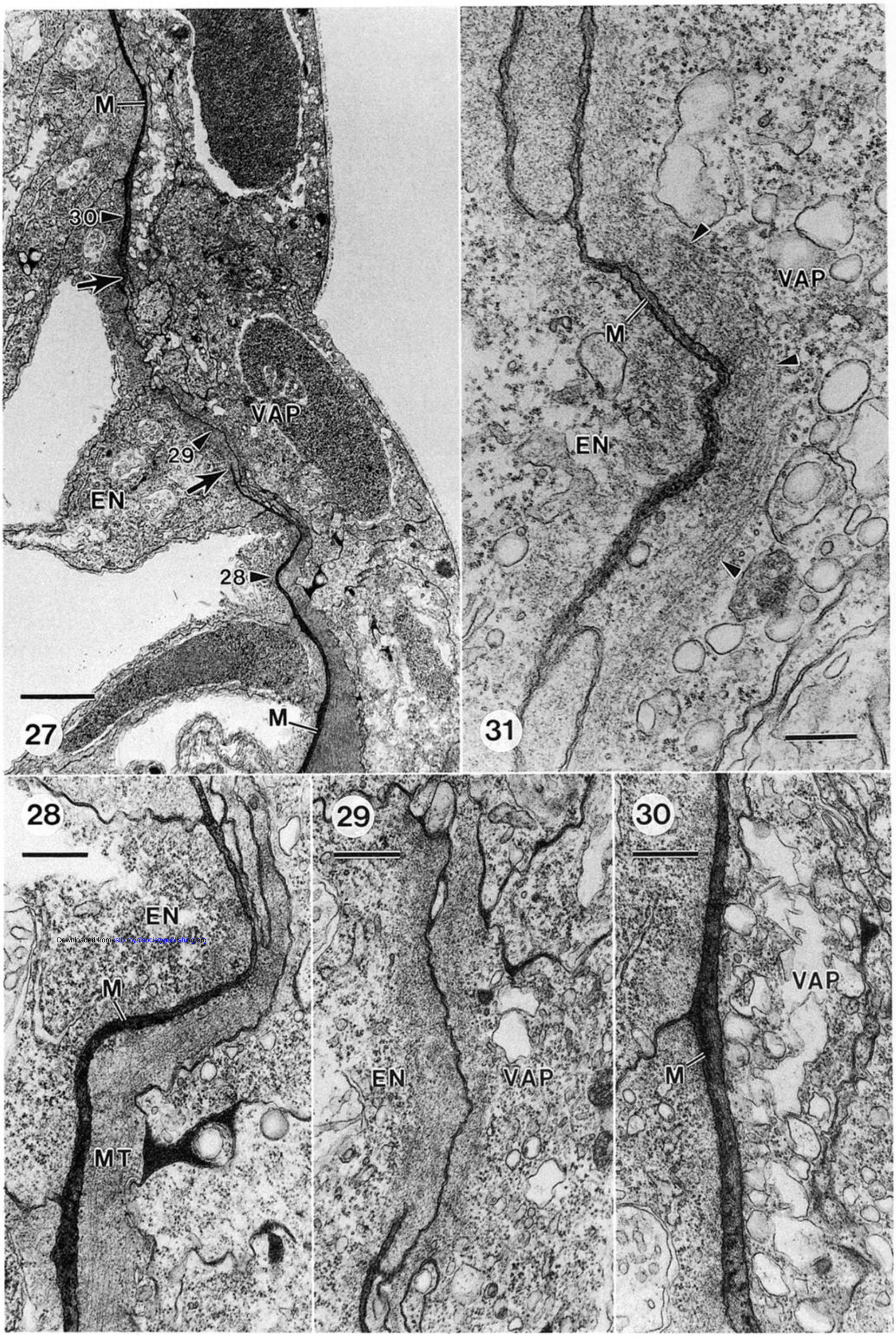

gure 27. Longitudinal section through autotomy plane of pinched intact tentacle showing large hole in mesoglea M; edges of hole marked by arrows) underlying vacuolated autotomy plane cell (VAP). Also note peripheral ngitudinal extension of endoderm cells adjacent to mesogleal hole. Enlargements of regions indicated by numbered rowheads are shown in figures 28, 29 and 30, respectively. Scale bar 2 μm.

gure 28. Mesoglea (M) underlying a muscle tail (MT) on distal side of mesogleal hole. EN, endoderm. Scale bar 5 μm.

gure 29. Endodermal cell (EN) juxtaposed to VAP cell with no intervening mesoglea. Note absence of vacuoles ong basal membrane of VAP cell. Scale bar 0.5 μm.

gure 30. Mesoglea (M) just proximal to the mesogleal hole with overlying VAP cell containing vacuoles adjacent the basal membrane bordering the mesoglea. Scale bar 0.5 μm.

gure 31. Thin, although still intact, area of mesoglea (M) within autotomy plane of a pinched intact tentacle. A ltwork of microtubules and microfilaments (arrowheads), rather than vacuoles borders the basal membrane of verlying VAP cell. EN, endoderm. Scale bar 0.3 μm.

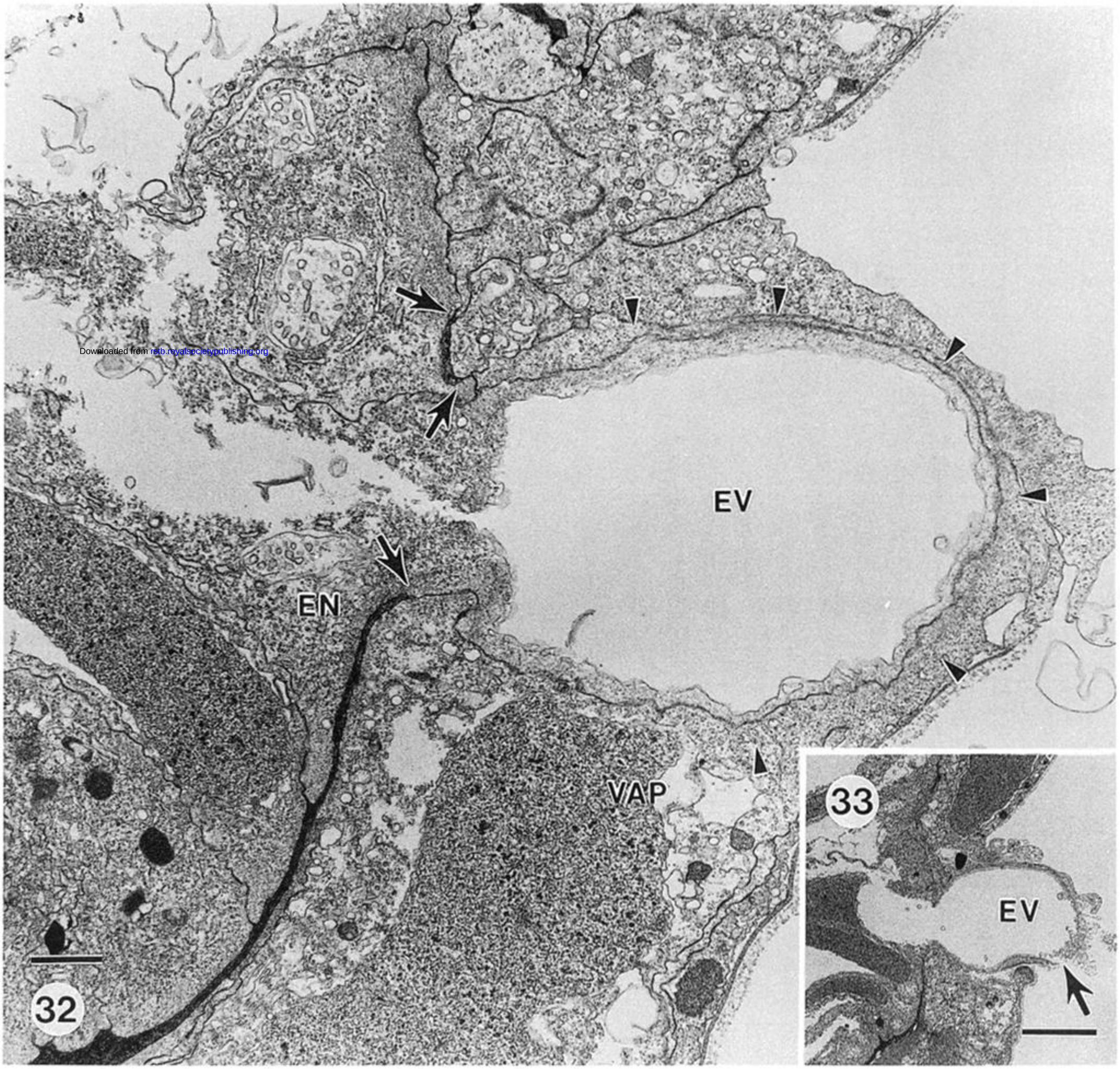

gure 32. Longitudinal section of autotomy plane from a pinched intact tentacle showing where the cytoplasmic rind an endodermal cell (EN), along with its central vacuole (EV) has punched through a hole in the mesoglea (broken ges of mesoglea indicated by arrows) into the overlying VAP cell. There are no vacuoles within the thin layer of AP cell cytoplasm (arrowheads) overlying the endodermal outpocketing. Scale bar 1 μm.

gure 33. Same area as figure 32 taken from a subsequent section. The outpocketed endodermal vacuole (EV) has oken through the overlying ectoderm at site marked by the arrow. Scale bar 5 μm.

PHILOSOPHICAL TRANSACTIONS OF THE ROYAL SOCIETY B BIOLOGICAL SCIENCES